

Critical Benchmarking of Popular Composite Thermochemistry Models and Density Functional Approximations on a Probabilistically Pruned Benchmark Dataset of Formation Enthalpies

Sambit Kumar Das,¹ Sabyasachi Chakraborty,¹ and Raghunathan Ramakrishnan^{1, a)}
Tata Institute of Fundamental Research, Centre for Interdisciplinary Sciences, Hyderabad 500107, India

(Dated: 29 December 2020)

First-principles calculation of the standard formation enthalpy, ΔH_f° (298 K), in such large scale as required by chemical space explorations, is amenable only with density functional approximations (DFAs) and certain composite wave function theories (cWFTs). Alas, the accuracies of popular range-separated hybrid, ‘rung-4’ DFAs, and cWFTs that offer the best accuracy-vs.-cost trade-off have until now been established only for datasets predominantly comprising small molecules; their transferability to larger systems remains vague. In this study, we present an extended benchmark dataset of ΔH_f° for structurally and electronically diverse molecules. We apply quartile-ranking based on boundary-corrected kernel density estimation to filter outliers and arrive at Probabilistically Pruned Enthalpies of 1,694 compounds (PPE1694). For this dataset, we rank the prediction accuracies of G4, G4(MP2), ccCA, CBS-QB3 and 23 popular DFAs using conventional and probabilistic error metrics. We discuss systematic prediction errors and highlight the role an empirical higher-level correction (HLC) plays in the G4(MP2) model. Furthermore, we comment on uncertainties associated with the reference empirical data for atoms and the systematic errors stemming from these that grow with the molecular size. We believe these findings to aid in identifying meaningful application domains for quantum thermochemical methods.

Keywords: thermochemistry, composite methods, density functional theory, formation enthalpies

I. INTRODUCTION

An unmet promise in ab-initio quantum chemistry is to predict molecular and reaction enthalpies with such high an accuracy, that reaction energies and relative stabilities of constitutional/conformational/geometric isomers can be established in agreement with experimentally observed trends—but at a computational cost that is comparable to that of a density functional approximation (DFA) with a reasonably converged basis set^{1,2}. This situation is apparent in the context of emerging data science campaigns, where computational explorations and statistical inference of molecular properties across *chemical compound space* is the prime focus^{3–8}. Arguably, one of the most sought-after molecular properties for data-mining is the standard formation enthalpy, ΔH_f° (298 K), because of its significance to energetics and rates of industrial^{9,10} and atmospheric chemical reactions^{11,12}. Hence, development of a rapid thermochemistry protocol demonstrating a faithful transferability of accuracy—from that of the molecules used for the method’s calibration (*i.e. training*)—to a *new* molecule with arbitrary stoichiometry/valency and non-standard bond distances/angles will remain an active research domain^{13–15}.

Karton classified the most widely used composite wavefunction theories (cWFTs) into those involving a

post-CCSD(T)-level energy correction and those requiring a CCSD(T)-level treatment¹⁶. The former includes: W4¹⁷, HEAT-345QP¹⁸, and HEAT-456QP¹⁹ which depend on higher-order terms in the coupled-cluster expansion (*i.e.* quadruple, quintuple and higher excitations) to forecast molecular energies of ‘high chemical accuracy’, with prediction error ≤ 1 kJ/mol^{20,21}. Alas, the severe computational complexities of these methods restrict their applicability to small molecules with at most a few dozen electrons. The latter category of thermochemistry methods is dependent on electron correlation energy estimated at the relatively less intensive CCSD(T)-level, where the triples contribution is included perturbatively. Such a compromise extends the application domain of this class of methods—for instance, CBS-QB3²², G4²³, ccCA^{24–26} and their offshoots—to larger molecules with up to a couple of dozen main group atoms. Depending on the size of the basis set with which the CCSD(T) energy is estimated, cWFTs can yield an average prediction accuracy in the $\approx 1 - 2$ kcal/mol range¹⁶. It must be noted that based on the computational complexities of these approaches, which scale unfavorably with molecular size, their application domain is restricted to molecules of size CF₄ or CH₃COOH for FCI/CBS based methods, C₆H₆ or C₆H₁₄ for CCSDT(Q)/CBS based methods, C₂₀H₂₀ for CCSD(T)/CBS methods, while CCSD(T)/TZ based methods can handle large systems like C₆₀.

A number of data-driven computational chemistry benchmark studies have explored subsets of the GDB17 molecular universe²⁷ comprising 166,443,860,262 (*i.e.*

^{a)}Electronic mail: ramakrishnan@tifrh.res.in

166.4 billion) closed-shell, organic molecules each containing up to 17 atoms of C, N, O, S, and halogens. These high-throughput computational studies have catered the data requirements of methodological studies focusing on machine learning (ML) modeling^{28,29}. For instance, a past study computed DFT-level structures and properties of a small subset of the GDB17 dataset with 133,885 small organic molecules (the QM9 dataset), each containing up to nine C, O, N and F atoms^{30,31}. Recently, the QM9 dataset was subjected to rigorous G4(MP2) treatment to estimate total energies, atomization energies and standard enthalpies of formation^{5,32}. Other studies^{33,34} have extended these works by applying ML and Δ -ML³¹ to statistically infer G4(MP2)-level energies of a small set of organic molecules containing more than 9 heavy atoms. On the basis of dataset size alone, these studies represent some of the massive high-throughput quantum chemistry efforts ever undertaken. However, it remains to be seen if QM9 molecules' ΔH_f° values predicted with G4(MP2) are quantitatively accurate to a degree that is relevant for comparison with experiments.

The complexity involved in validating computed results in chemical space explorations is twofold: Firstly, it is a non-trivial task to automate the collection and pruning of available experimental energies for such a large dataset as QM9. Secondly, even if all these molecules are 'synthetically feasible', only a tiny fraction have been plausibly characterized by gas phase measurements. Seemingly, the only viable way of probing the transferability of a computational method to unexplored regions in the chemical space is to benchmark on compounds of similar chemical composition. In this context, Narayanan *et al.*⁵ selected experimental values of ΔH_f° for 459 closed-shell hydrocarbons and their substituted analogues—containing atoms similar to those in QM9—from Pedley's extensive compilations^{35,36} and observed an average prediction error of 0.8 kcal/mol for G4(MP2). This value is comparable to that of G4(MP2)'s³⁷ and ccCA's³⁸ mean errors noted for similar molecules in the G3/05 small molecules dataset³⁹. However, such high prediction accuracies are not expected to hold for electronically and structurally more diverse molecules that can be combinatorially generated from the QM9 set by protonation, deprotonation, or iso-valence-electronic substitutions. For instance, Schwilk *et al.*⁴⁰ have selected about 4,000 molecules from the QM9 set and derived from this subset a new dataset QMspin, comprising 8000 triplet and 5000 singlet carbene compounds. To gain insight on the applicability of G4(MP2) to such non-trivial chemical subspaces, it is a timely pursuit to benchmark widely employed cWFTs on larger, curated benchmark datasets by extending upon existing thermochemistry benchmark sets.

In this study we aim to: (i) collect reference ΔH_f° values from several previous reports, and include new benchmark datasets containing experimental results

and present a consolidated dataset, (ii) apply a probabilistic procedure based on the best theoretical method applicable to the entire set to detect and eliminate potential outliers, (iii) report on the prediction errors based on mean and percentiles metrics for the cWFTs, G4, G4(MP2), ccCA, and CBS-QB3 along with 23 popular DFAs and 2 semi-empirical methods, (iv) comment on the transferability of empirical corrections in G4(MP2) to the pruned ΔH_f° dataset presented here, (v) from the larger dataset presented, identify and study a new benchmark set with isomerization reaction enthalpies, and (vi) finally, inspect the uncertainties in thermochemistry calculations arising due to the use of empirical reference data for atoms. A general theme of our analyses is to shed more light on the transferability of the G4(MP2) method that offers a suitable cost-accuracy trade-off for sampling across small molecules chemical spaces such as GDB17²⁷.

II. COMPUTATIONAL DETAILS

Thermochemistry calculations with G4(MP2), ccCA and DFAs were automated through *in-house* scripts which rely on ORCA^{41,42}. Of the many ccCA variants developed by Wilson *et al.*^{24,25,38,43–45}, this work explores ccCA-P²⁵. G4 and CBS-QB3 calculations were carried out with Gaussian-16 suite of programs⁴⁶. PM6⁴⁷ and PM7⁴⁸ calculations were done via MOPAC⁴⁹. We considered 23 DFAs from various levels of Perdew's 'Jacob's ladder'⁵⁰: generalized gradient approximation (GGA)—BLYP⁵¹, PW91⁵² and PBE⁵³; hybrid GGA—B3LYP⁵⁴, O3LYP⁵⁵, X3LYP⁵⁶ and PBE0⁵⁷; meta-GGA—TPSS⁵⁸; hybrid meta-GGA—TPSS0⁵⁹ and M06-2X⁶⁰. We also selected the range-separated hybrid functionals: CAM-B3LYP⁶¹, ω B97X⁶², ω B97X-D3⁶³, ω B97X-V⁶⁴, ω B97M-V⁶⁵, ω B97X-D3BJ, and ω B97M-D3BJ, where Grimme's D3 dispersion with Becke-Johnson damping (D3BJ)^{66–69} has been included explicitly. Furthermore, B2PLYP⁷⁰, B2PLYP-D3⁷¹ and mPW2PLYP-D⁷² represent the double-hybrid functionals considered in this study, some of which include dispersion corrections. Additionally, we also benchmarked a few of the aforesaid functionals with an additional dispersion correction, namely, B3LYP-D3, TPSS0-D3 and M06-2X-D3.

Initial geometries of molecules from previously studied datasets were collected from their corresponding sources—when such information was available—and subjected to geometry relaxations. For compounds with no previously reported geometries, we consulted popular online chemical databases: NIST⁷³, ChemSpider⁷⁴ and Pub-Chem⁷⁵. In some cases, we created initial geometries using the software Avogadro⁷⁶ and carried out minimum energy geometry relaxation with universal forcefield (UFF)⁷⁷. We performed DFA calculations at the B3LYP/6-31G(2df,p) minimum energy ge-

ometry in a single point fashion using the def2-QZVP basis set, which has been shown to yield predictions close to the Kohn-Sham limit⁷⁸. PM6 and PM7 calculations were performed using precise geometry relaxation thresholds at the corresponding levels. Geometry optimizations with DFAs were carried out with tight convergence criteria with 10^{-4} as the threshold for the maximum component of the force vector. To facilitate convergence of the geometry towards the energy minimum, force constants were computed at every fifth step of geometry optimization. In all calculations, SCF convergence was attained with `verytightscf` criteria corresponding to a threshold of 10^{-9} Hartree for the total energy. For the numerical quadrature of the exchange correlation part of the energy in DFAs, we used Lebedev-434 angular grids and Grid7 settings for Gauss-Chebyshev radial grids. From the zero-point corrected electronic energy, ΔH_f° (298K) was calculated according to the standard convention⁷⁹. Heats of formation of atoms at 0 K, $\Delta H_f^\circ(0\text{ K})$, and enthalpy corrections, for elements in their standard states, $H^\circ(298\text{ K}) - H^\circ(0\text{ K})$ are listed in APPENDIX. Spin-orbit corrections to the electronic energies of atoms, ions, selected diatomic molecules⁸⁰ and acetylene were collected from Refs. 23, 81, and 82.

III. BENCHMARK DATASET OF MOLECULAR STANDARD FORMATION ENTHALPIES

We gathered benchmark values of ΔH_f° from six previously studied datasets amounting to 2,204 entries:

1. G3/05 dataset³⁹ is a set of 454 energies distributed into: 270 ΔH_f° , 105 ionization energies (IE), 63 electron affinities (EA), 10 proton affinities (PA), and 6 binding energies (BE) of hydrogen-bonded complexes. This set has been extensively used in the development of the G_n theories and also for validating other *ab initio* thermochemical protocols. We note in passing that in the 270 subset only 247 are ΔH_f° values, the remaining 23 are atomization energies that we excluded.
2. Alexandria dataset⁸³ contains classes of molecules similar to that of G3/05 but many in number with diverse molecular sizes, thus, providing a platform to examine the transferability of methods that perform well for G3/05. Out of 2,704 entries in this dataset, 1,383 compounds that contain experimental values of ΔH_f° have been selected.
3. Pedley CHONF is a set derived from 459 experimental values for hydrocarbons and substituted hydrocarbons from Pedley’s report³⁶ containing the atoms H, C, N, O, and F. An earlier study⁵ benchmarked the accuracy of G4(MP2) for this

dataset and reported an average prediction error of 0.8 kcal/mol.

4. ISO-8 comprises experimental isomerization energies and the corresponding ΔH_f° for 8 sets of constitutional isomers amounting to 64 entries⁸⁴.
5. CBH-Rad49⁸⁵ contains 49 cyclic & acyclic radicals with reference ΔH_f° energies gathered from experiment and high-level theoretical modeling. From this set, we collect 18 experimentally determined entries.
6. ΔH_f° of 33 adamantanes estimated by a simultaneous least-squares regression involving a thermochemical network of 300 isodesmic reactions⁸⁶.

To further enrich the benchmark set collected from previous findings, we included 521 compounds from Refs. 35 and 36 that have never been subjected to theoretical modeling. These compounds belong to the following three categories: cyclic hydrocarbons, halogen-rich hydrocarbons and constitutional isomers with 17 unique stoichiometries (ISO-17). The number of compounds added from each of the aforesaid dataset is shown in Fig. 1. The total number of compounds from the collective set amounts to 2,725, where we detected a number of repeated entries. To eliminate redundant entries, we followed a systematic data-deduplication procedure based on stoichiometries, principal moments of inertia and counts of heavy atom bonds. Firstly, we separated radicals from non-radicals, and binned entries in each category appropriately based on stoichiometries. Following this, we clustered constitutional isomers for a given stoichiometry based on canonical smiles and principal moments of inertia of every molecule; each cluster is considered as a set of redundant entries. Finally, for each cluster, the average experimental value was calculated and the conformer with the least G4(MP2) value; for ambiguous cases, we used G4 results.

Following de-duplication, 2,725 entries reduced to 1,796 unique entries, for which it is a non-trivial task to quantify—*ab initio*—plausible uncertainties arising from random and systematic errors in the experimental measurements. Paulechka *et al.*⁸⁷ discussed the reasons for typical uncertainties in experimentally determined ΔH_f° and indicated that such deviations can amount to even a few kJ/mol. In that study, for very critical benchmarking of DLPNO-CCSD(T) ΔH_f° , the authors selected 45 compounds with at least two independent experimental results. Even when using such ‘precise’ experimental values as references, error trends based on the mean unsigned error (MUE) can severely underestimate thermochemical uncertainty⁸⁸. Simm *et al.*⁸⁹ have discussed how a performance analysis based on MUE is prone to fail as it does not distinguish the systematic contributions to the errors from the non-systematic counterparts. For pathological error distributions, arising plausibly due to the presence of outliers in the reference

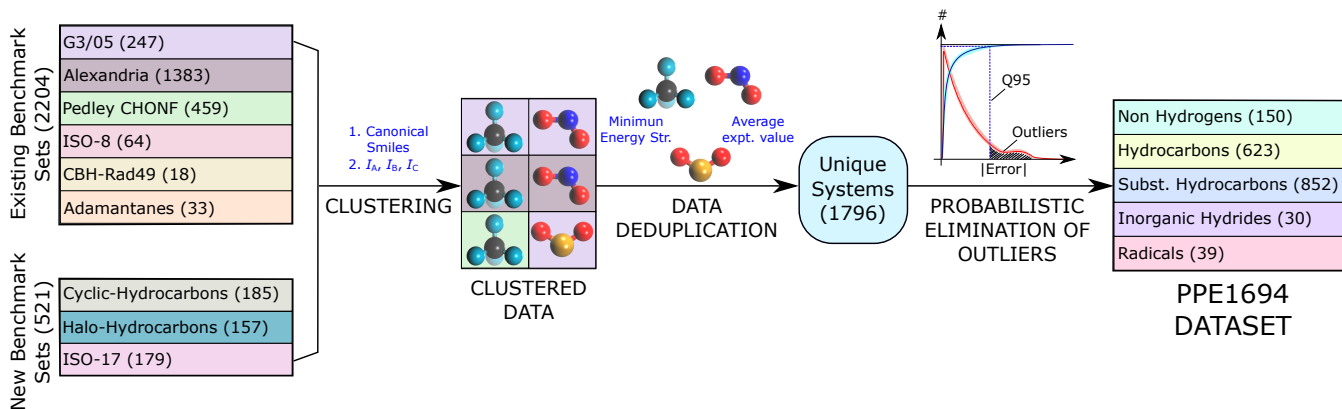


FIG. 1. PPE1694 dataset of molecular standard formation enthalpies: Data collection, deduplication and probabilistic filtering of outliers. See text for more details of the individual datasets and their sources.

dataset, prediction uncertainties can be truncated using percentile-based error metrics^{88,90–92}. More specifically, performance ranking of *ab initio* methods revealing trends in uncertainties has been made possible by the use of the 95th percentile of the absolute intensive (*i.e.* normalized) error distributions along with the MUE⁹³. It is the subject of Section IV to discuss a procedure to detect probabilistic tendencies of an entry from the 1,796 set to be an outlier.

IV. PROBABILISTIC PRUNING OF THE DATASET

For the duplicate-free 1,796 set, we utilize a probabilistic argument to detect outliers. The principle behind this scheme is to use highly accurate computed values of ΔH_f° as references and mark only those molecules that lie beyond the 95th percentile of the error distribution as outliers. The cumulative probability used for this purpose acts as a *prior* distribution—more robust the reference, more reliable the prior is. Hence, it may be anticipated that this scheme is guaranteed to detect genuine outliers when one of the high-precision methods such as W4, HEAT-456QP, or HEAT-345QP is used as a reference. Given the size of majority of the molecules in the dataset, we depend on G4 values to define the prior probability. For 20 electron-rich systems in the 1,796 set, for which G4 calculations were not amenable, we relied on G4(MP2).

We begin with absolute errors in G4-predicted ΔH_f° for the 1,796 set. Following the arguments presented by Savin *et al.*⁹⁴ and Perdew *et al.*⁹⁵, and selected an intensive error measure to account for the fact that the dataset contains molecules spanning various sizes. For this purpose, we used MUE per valence electron, to capture periodic trends in molecular thermochemistry. From discrete values of the G4 error, we obtained a continuous probability distribution using the boundary corrected kernel density estimation (bc-KDE), where a radial ba-

sis function is expanded at each discrete value. In KDE, we take a kernel in the form of the standard normal distribution $\mathcal{N}(0, 1)$

$$K_h(x - x_i) = \frac{1}{\sqrt{2\pi}h} \exp\left[-\frac{(x - x_i)^2}{2h^2}\right], \quad (1)$$

where K_h is the normalized estimator. A kernel function is expanded at every data point, giving rise to the (un-normalized) total density function that is an average of all kernels

$$\hat{f}(x, h) = \frac{1}{N} \sum_{i=1}^N K_h(x - x_i) \quad (2)$$

It is a well-known problem that KDE can delocalize beyond the allowed domain; in such cases, the naive approach of truncating the total density function $f(x)$ often underestimates the actual probability distribution. This effect is illustrated using a toy dataset in Fig. 2. To this end, we employ boundary-corrected kernels of the form

$$K_h^{\text{bc}}(x - x_i) = [K_h(x - x_i) + K_h(x + x_i - 2x^*)] \mathbf{1}_{x \in A}, \quad (3)$$

where the indicator function $\mathbf{1}_{x \in A}$ is 1 when $x \in A$ and vanishes otherwise⁹⁶. Bc-KDE captures the true nature of the probability density when the property is bounded. While the individual kernel functions that cross the boundary are truncated by the indicator function, the total probability is still conserved through a normalization of the resulting probability density, see Eq. 5.

In our bc-KDE calculations, we used a kernel width of 0.005 kcal/mol and determined the total density function as the average

$$\hat{f}(x, h) = \frac{1}{N} \sum_{i=1}^N [K_h(x - x_i) + K_h(x + x_i - 2x^*)] \mathbf{1}_{x \in A}, \quad (4)$$

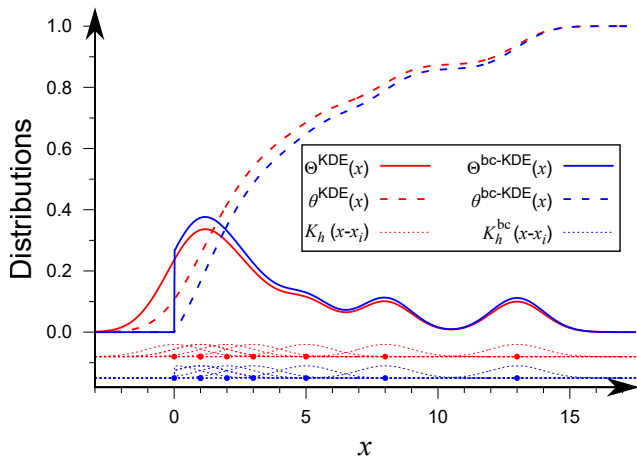


FIG. 2. Probability density function, $\theta(x)$, and cumulative distribution function, $\Theta(x)$, based on kernel density estimation (KDE) and its boundary corrected analog, bc-KDE, demonstrated for an exemplary dataset with eight points: $x_1 = 0$, $x_2 = x_3 = 1$, $x_4 = 2$, $x_5 = 3$, $x_6 = 5$, $x_7 = 8$ and $x_8 = 13$. For clarity, $\theta(x)$ has been multiplied by 100. Also shown in the bottom of the plot are the kernel basis functions $K_h(x - x_i)$ and $K_h^{bc}(x - x_i)$ centered at the data points with arbitrarily shifted ordinates.

which is normalized over the domain to give the probability density function (PDF)

$$\hat{\phi}(x) = \frac{\hat{f}(x, h)}{\|\hat{f}(x, h)\|_2}. \quad (5)$$

The cumulative density function (CDF) used to identify percentiles is obtained by integrating the PDF

$$\hat{\Phi}(x) = \int_A^B dx \hat{\phi}(x). \quad (6)$$

The resulting CDF enables statistical modeling of the probability to obtain a certain degree of prediction accuracy for a given quantum chemistry method as previously noted by Pernot *et al.*⁹⁰. To estimate the variance of the CDF, we followed bootstrapping with 1000 shuffles, with 500 points randomly sampled from the 1,796 set. The boundary-corrected kernel density probability distribution, θ^{bc-KDE} and the corresponding cumulative density function Θ^{bc-KDE} are on display in Fig. 3. To eliminate any sampling bias, we use the lower bound of the 95th percentile, denoted $Q95^-$ in Fig. 3, as a threshold; all compounds for which the MUE per valence electron is greater than $Q95^-$ are marked as outliers and eliminated from the dataset. We thus arrive at the benchmark set of probabilistically pruned enthalpies of 1,694 compounds, denoted henceforth PPE1694. For the original 1,796 set, MUE of G4(MP2) is 2.17 kcal/mol, for 1,776 entries G4’s MUE is 1.94 kcal/mol. For the pruned 1,694 set, G4(MP2)’s MUE is 1.70 kcal/mol. As

stated before, G4 calculations were not amenable to 20 electron-rich systems, hence for the collective reference set with 1,674 G4 and 20 G4(MP2) values, the MUE is 1.51 kcal/mol.

In Section VI D, we discuss how the performances of cWFTs and DFAs deteriorate systematically because of the uncertainties associated with empirical atomic parameters used for thermochemistry energetics. Compared to the small molecules benchmark set G3/05, PPE1694 covers the space of molecules that contain more atoms as well as more valence electrons; qualitative trends are illustrated in Fig. 4. The largest number of valence electrons in G3/05 and PPE1694 sets are 66 (C_6F_6 and C_6F_5Cl) and 166 ($C_{10}F_{18}$), respectively. On the other hand, the maximum number of atoms in a given compound is 26 (C_8H_{18}) for the G3/05 set, and 56 ($C_{18}H_{37}Cl$) for PPE1694. Both sets are dominated by closed-shell cases as evident from larger counts for compounds with even number of valence electrons, see Fig. 4a.

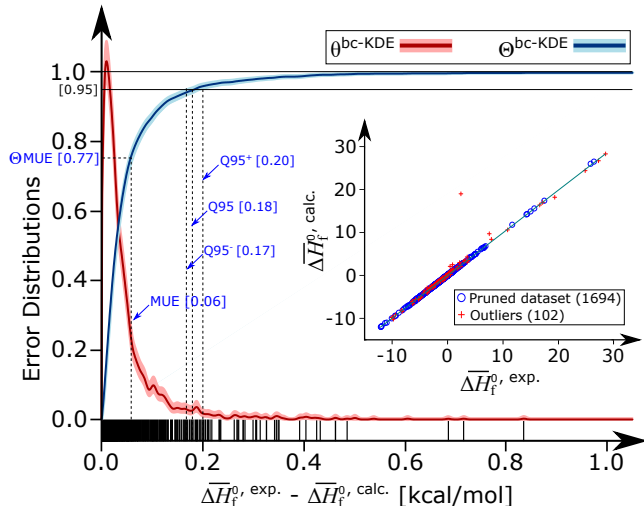


FIG. 3. Boundary-corrected kernel density probability distribution, θ^{bc-KDE} and the corresponding cumulative density function Θ^{bc-KDE} for the absolute deviations of the calculated ΔH_f^0 . Calculated results comprise G4 values for 1,674 small-to-medium systems, and G4(MP2) values for 20 electron-rich molecules. The overline indicates that the values are normalized over valence electrons. Uncertainty envelopes were determined by bootstrapping. The inset features a scatterplot.

V. DRESSED ATOM CORRECTIONS FOR SYSTEMATIC ERRORS IN DENSITY FUNCTIONAL APPROXIMATIONS

It is well known that DFA predicted ΔH_f^0 suffer systematic errors through insufficient modeling of atomization energies. Such errors can be empirically corrected either through a quasi-atom correction scheme^{59,97} or by

a bond density function approach⁹⁸. The latter method captures the atomic local environment in terms of chemical bonds yielding a parameterization guided by the unique chemistry of the molecule. However, this often results in overfitting to a given dataset. Here, we rely on an additive quasi-atom correction scheme because of its inherent robustness and simplicity. Accordingly, DFA predicted ΔH_f° is corrected by a sum of element-specific constant

$$\Delta H_f^\circ(\text{exp.}) = \Delta H_f^\circ(\text{DFA}) + \sum_i c_i n_i, \quad (7)$$

where c_i is the correction for the i -th atom-type while n_i is the number of such atoms in the molecule. From PPE1694, we randomly selected 300 entries ensuring all elements were represented at least twice. This set was hence used to determine the element-wise coefficients through a least-squares regression. Coefficients for all 22 unique elements present in PPE1694 are available, for 23 DFAs studied here, on the Supplementary Information page <http://moldis.tifrh.res.in/data/prunedHOF>.

VI. RESULTS AND DISCUSSIONS

A. Benchmark results for cWFTs and DFAs

While cWFTs are the recommended choice for modeling ΔH_f° , the favorable accuracy-to-speed trade-offs of DFAs have facilitated ΔH_f° predictions for large molecules through isodesmic reaction schemes^{99,100} and group additivity schemes¹⁰¹. A benchmark across popular DFAs on a curated dataset such as PPE1694 (see Fig. 4) may provide insights into how the performances of these methods can be refined through proper selection of basis sets and additional dispersion corrections. To this end, we embark upon comprehensive benchmarking of G4, G4(MP2), ccCA, CBS-QB3, 23 popular DFAs, as well as the semi-empirical methods, PM6 and PM7.

Table I summarizes MUEs, RMSEs and maximum signed errors for each method across various classes of compounds. It is apparent while moving across the subsets that the performance of cWFTs—G4, G4(MP2), and ccCA—are consistent irrespective of the compound type, with total MUEs ≤ 1.70 kcal/mol. CBS-QB3 performs poorly relative to other cWFTs, notably for non-hydrogens with an MUE over 6 kcal/mol.

We note the GGA functionals to consistently underperform across all subsets. A closer look reveals errors to be mostly systematic as larger MUEs are usually encountered for subsets with greater structural complexities. Hybrid GGAs mostly improve upon GGA with PBE0 showing the best performance. This is because hybrid GGAs are designed to correct for the spurious self-interaction error in semi-local DFAs^{102–104}. Overall,

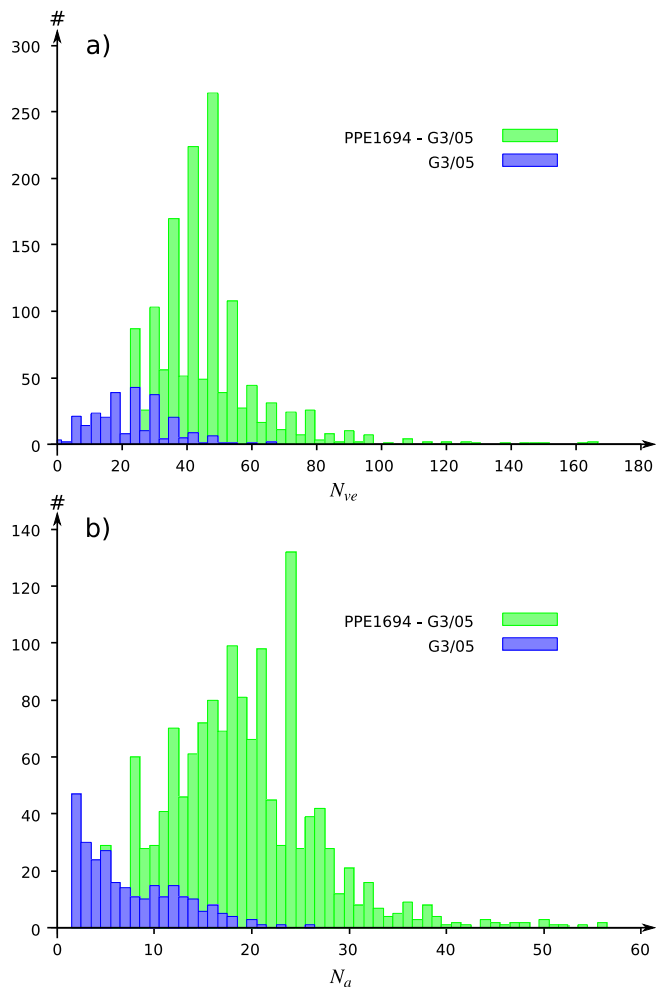


FIG. 4. Distribution of compounds in the G3/05 dataset compared to other molecules that are present in PPE1694: a) Counts for number of valence electrons N_{ve} , b) Counts for number of atoms N_a .

as we move up the *Jacob's ladder*⁵⁰, we observe a consistent drop in MUE. Most notably, we find the performance of long-range tuned hybrid DFAs on par with double hybrid ones. The importance of capturing long-range effects can be further understood by noting that explicit inclusion of an empirical dispersion correction overall improves the performance of most DFAs. Semi-empirical methods PM6 and PM7 under-perform across all subsets except for hydrocarbons and substituted hydrocarbons, where their accuracy is on par with long-range tuned functionals with PM7 slightly outperforming PM6.

For the Top-6 methods: G4, G4(MP2), ccCA, CBS-QB3, ω B97M-D3BJ, and ω B97M-V, we have graphically summarized the error metrics in Fig. 5. As noted in Table. I, G4 ranks best followed by G4(MP2) and ccCA, both exhibiting comparable accuracies. In terms of the maximum absolute deviation (Max), ccCA seems slightly better than G4 and G4(MP2) for inorganic hydrides. Barring radicals, ω B97M-D3BJ performs slightly

TABLE I. Prediction errors in the modeling of ΔH_f° . For selected cWFTs, DFAs and semi-empirical methods, mean unsigned error (MUE) is reported for each class of compounds in the PPE1694 benchmark dataset. The root-mean-square-error is given in parenthesis while, the most positive and negative errors are provided inside a square bracket. All values are in kcal/mol.

Methods	Nonhydrogens (150)	Hydrocarbons (623)	Subst. hydrocarbons (852)	Inorganic hydrides (30)	Radicals (39)	Total (1,694)
G4(MP2)	2.21 (3.31) [-12.33, 11.15]	1.81 (2.80) [-10.47, 18.08]	1.57 (2.15) [-7.25, 9.81]	0.85 (1.20) [-4.15, 1.96]	1.37 (1.88) [-3.35, 5.31]	1.70 (2.50) [-12.33, 18.08]
G4 ^f	1.95 (2.97) [-11.05, 11.73]	1.51 (2.32) [-10.75, 11.02]	1.40 (1.98) [-7.06, 9.16]	0.98 (1.25) [-3.87, 1.65]	1.13 (1.49) [-3.45, 3.47]	1.47 (2.18) [-11.05, 11.73]
ccCA ^b	2.15 (3.24) [-12.54, 10.50]	1.69 (2.43) [-9.60, 19.71]	1.58 (2.18) [-9.36, 8.67]	1.00 (1.27) [-2.52, 2.99]	1.59 (2.25) [-5.88, 1.03]	1.66 (2.37) [-12.54, 19.71]
CBS-QB3 ^c	6.29 (8.87) [-14.88, 31.23]	2.75 (3.41) [-15.99, 6.76]	2.32 (3.38) [-6.74, 17.25]	2.87 (4.41) [-17.14, 9.63]	1.70 (2.20) [-6.00, 2.82]	2.82 (4.17) [-17.14, 31.23]
BLYP	7.22 (11.37) [-40.86, 38.13]	7.53 (11.63) [-74.83, 16.85]	6.24 (9.93) [-77.27, 10.34]	4.19 (6.19) [-24.98, 8.43]	6.35 (8.42) [-27.01, 10.91]	6.77 (10.63) [-77.27, 38.13]
PW91	6.02 (8.53) [-25.20, 35.93]	3.06 (4.44) [-27.32, 9.77]	3.74 (5.23) [-29.15, 8.49]	4.35 (5.69) [-15.72, 10.56]	3.58 (4.30) [-8.18, 9.51]	3.70 (5.33) [-29.15, 35.93]
PBE	6.26 (8.80) [-25.67, 36.33]	3.07 (4.42) [-26.75, 9.77]	3.93 (5.47) [-29.14, 8.09]	4.53 (6.02) [-16.35, 11.30]	3.70 (4.47) [-7.89, 9.89]	3.83 (5.49) [-29.14, 36.33]
TPSS	6.18 (9.15) [-31.67, 34.61]	4.75 (7.15) [-44.02, 11.08]	5.01 (7.22) [-46.26, 7.44]	5.18 (6.93) [-19.76, 13.62]	4.48 (5.54) [-13.10, 10.60]	5.01 (7.35) [-46.26, 34.61]
B3LYP	4.67 (7.05) [-26.39, 18.00]	6.11 (9.16) [-55.34, 10.12]	3.68 (6.30) [-55.38, 7.48]	2.55 (3.57) [-12.54, 5.43]	4.75 (6.25) [-19.85, 8.29]	4.67 (7.51) [-55.38, 18.00]
B3LYP-D3	3.71 (5.27) [-15.76, 17.90]	3.34 (4.95) [-26.15, 11.83]	2.45 (3.65) [-25.26, 9.37]	2.24 (3.10) [-10.08, 6.03]	3.49 (4.30) [-11.22, 6.47]	2.91 (4.33) [-26.15, 17.90]
O3LYP	4.81 (6.56) [-19.77, 21.05]	3.60 (4.88) [-28.19, 11.15]	3.00 (4.10) [-23.34, 11.24]	3.46 (4.44) [-8.55, 8.02]	2.97 (3.98) [-10.82, 9.70]	3.39 (4.66) [-28.19, 21.05]
X3LYP	4.34 (6.34) [-22.66, 16.34]	5.70 (8.54) [-51.25, 9.49]	3.31 (5.70) [-50.92, 8.01]	2.45 (3.36) [-11.22, 5.37]	4.56 (5.92) [-18.44, 8.10]	4.29 (6.91) [-51.25, 16.34]
PBE0	3.91 (5.22) [-12.84, 18.56]	3.17 (4.14) [-21.31, 10.39]	2.34 (3.17) [-13.38, 10.61]	2.79 (3.76) [-8.08, 7.22]	3.11 (3.83) [-9.22, 10.47]	2.81 (3.79) [-21.31, 18.56]
TPSS0	4.00 (5.34) [-17.61, 17.57]	4.47 (5.96) [-30.93, 8.85]	2.86 (3.96) [-26.08, 9.71]	3.64 (4.36) [-7.34, 8.62]	4.15 (4.66) [-5.94, 10.30]	3.60 (4.93) [-30.93, 17.57]
TPSS0-D3	3.53 (4.80) [-12.30, 18.25]	3.13 (3.91) [-14.30, 17.48]	2.24 (2.97) [-11.33, 12.05]	3.68 (4.29) [-6.76, 9.21]	3.44 (4.01) [-6.77, 9.82]	2.73 (3.58) [-14.30, 18.25]
M06-2X	2.99 (4.15) [-12.77, 14.39]	3.45 (4.31) [-21.81, 6.78]	2.52 (3.43) [-11.49, 16.40]	1.51 (1.97) [-5.63, 3.93]	2.11 (2.86) [-7.83, 6.43]	2.88 (3.81) [-21.81, 16.40]
M06-2X-D3	3.01 (4.18) [-12.80, 14.39]	3.29 (4.08) [-19.70, 7.03]	2.51 (3.42) [-9.75, 16.57]	1.51 (1.97) [-5.62, 3.92]	2.11 (2.84) [-7.69, 6.35]	2.81 (3.72) [-19.70, 16.57]
ω B97X	2.90 (3.97) [-10.54, 16.67]	2.38 (3.16) [-15.27, 11.30]	1.86 (2.47) [-7.84, 12.19]	2.13 (2.67) [-5.09, 6.38]	2.38 (3.10) [-7.33, 10.27]	2.16 (2.91) [-15.27, 16.67]
ω B97X-D3	3.00 (4.09) [-11.41, 17.44]	2.28 (2.97) [-13.06, 11.06]	1.86 (2.46) [-8.13, 11.17]	2.08 (2.60) [-5.70, 5.72]	2.31 (2.99) [-7.42, 9.70]	2.13 (2.85) [-13.06, 17.44]
ω B97X-V	3.28 (4.75) [-11.04, 20.83]	2.74 (3.49) [-12.27, 15.93]	2.11 (2.91) [-7.04, 14.40]	2.55 (3.20) [-5.72, 8.76]	2.44 (3.43) [-7.98, 12.78]	2.46 (3.35) [-12.27, 20.83]
ω B97X-D3BJ	3.35 (4.57) [-11.02, 17.52]	2.56 (3.29) [-12.88, 14.51]	2.04 (2.74) [-7.39, 12.01]	2.48 (3.02) [-5.96, 7.80]	2.21 (2.98) [-8.04, 9.14]	2.36 (3.16) [-12.88, 17.52]
ω B97M-V ^d	2.70 (3.92) [-11.32, 14.93]	2.03 (2.74) [-13.43, 9.06]	1.74 (2.36) [-6.51, 12.83]	1.48 (1.99) [-5.16, 4.53]	1.62 (2.35) [-7.70, 6.11]	1.92 (2.65) [-13.43, 14.93]
ω B97M-D3BJ ^d	2.71 (3.73) [-11.17, 15.12]	1.86 (2.65) [-13.91, 7.07]	1.64 (2.21) [-7.25, 11.49]	1.42 (1.79) [-4.11, 4.02]	1.71 (2.28) [-7.08, 3.73]	1.81 (2.53) [-13.91, 15.12]
CAM-B3LYP	3.25 (4.37) [-13.19, 16.21]	4.40 (6.18) [-32.27, 4.35]	2.44 (3.60) [-29.32, 11.32]	2.01 (2.46) [-4.72, 5.40]	3.44 (4.12) [-10.97, 7.59]	3.25 (4.77) [-32.27, 16.21]
B2PLYP	2.96 (4.58) [-15.82, 15.12]	3.44 (5.27) [-30.24, 5.63]	2.34 (3.70) [-29.70, 8.31]	1.92 (2.50) [-7.05, 3.88]	3.00 (3.92) [-12.40, 4.24]	2.81 (4.41) [-30.24, 15.12]
B2PLYP-D3	2.49 (3.88) [-12.61, 15.06]	2.39 (3.58) [-20.07, 13.23]	1.88 (2.67) [-15.29, 9.37]	1.73 (2.35) [-5.91, 3.89]	2.45 (3.15) [-9.14, 3.61]	2.13 (3.16) [-20.07, 15.06]
mPW2PLYP-D	2.34 (3.40) [-11.98, 13.89]	1.99 (2.96) [-15.63, 10.34]	1.68 (2.28) [-9.51, 9.22]	1.62 (2.07) [-4.70, 2.97]	2.29 (2.81) [-8.35, 3.78]	1.87 (2.67) [-15.63, 13.89]
PM6	7.81 (11.04) [-40.57, 24.09]	3.79 (5.36) [-11.99, 42.15]	3.10 (4.29) [-25.88, 19.44]	4.35 (5.21) [-8.52, 9.92]	12.88 (16.28) [-41.87, 37.50]	4.02 (6.10) [-41.87, 42.15]
PM7	9.34 (13.89) [-72.66, 32.44]	3.44 (4.58) [-16.95, 23.05]	2.83 (3.99) [-28.91, 15.79]	6.04 (9.29) [-14.44, 35.40]	11.93 (14.58) [-42.78, 25.76]	3.89 (6.26) [-72.66, 35.40]

^a Nonhydrogens: 141, Hydrocarbons: 615, Subst. hydrocarbons: 849, Total: 1,674

^b Nonhydrogens: 146, Hydrocarbons: 551, Subst. hydrocarbons: 805, Total: 1,571

^c Nonhydrogens: 147, Hydrocarbons: 621, Total: 1,689

^d Nonhydrogens: 139, Inorganic hydrides: 28, Total: 1,681

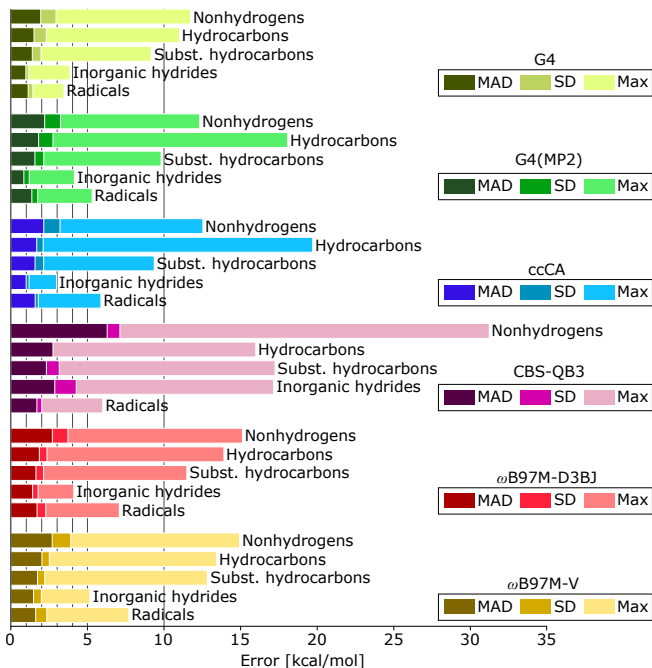


FIG. 5. Prediction errors in ΔH_f^0 across compound types and methods; MUE: mean unsigned error, SD: standard deviation, Max: maximum absolute deviation. For number of entries in each class of compounds and methods, see Table. I

better than ω B97M-V across the subsets. Both of them significantly outperform CBS-QB3.

A drawback of relying on mean-based error metrics is that, these do not provide a complete picture of the error distribution. For this purpose, percentile-based metrics have been shown to be more suitable (see Ref. 90 and references therein). Fig. 6 presents mean- and percentile-based metrics for all the computational methods studied here. A method with good prediction accuracy should show smaller MUEs as well as small values of Q_N , where $N > 50$. Spearman rank correlation (ρ) between two sets is a good indicator for qualitative agreement between them¹⁰⁵. Overall, methods with low Q_N or MUE, show $\rho \approx 1$. In general, we find dispersion corrections to improve the ρ of DFAs.

An examination of the compounds showing extreme (*i.e.* most-positive or most-negative) errors for a given computational method often reveals if the error is systematic or non-systematic in nature. For the latter to be evident one has to consider normalized or intensive errors such as error-per-electron or error-per-atom. In the case of G4(MP2), along with the total error, we also consider error-per-valence-electron and inspected those compounds exhibiting extreme errors (see Fig. 7). Barring hydrocarbons, we find the compounds with extreme intensive and extensive (*i.e.* unnormalized) error to mostly comprise heavy atoms. Predominant of the compounds with large intensive error are with fewer heavy atoms, while those with large extensive (or un-

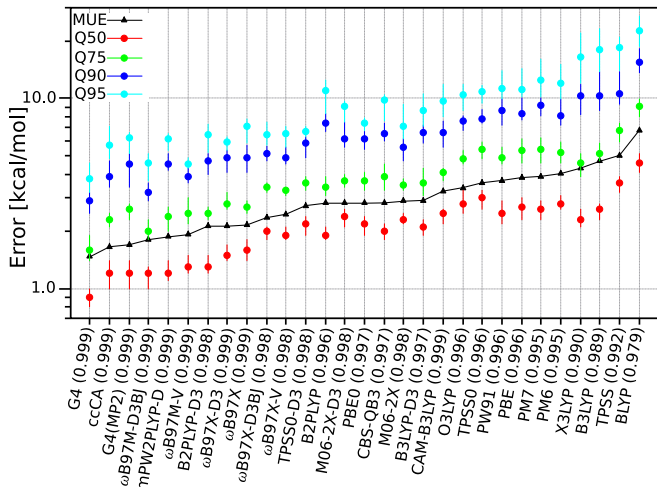


FIG. 6. Ranking of the prediction accuracy of cWFTs, DFAs and semi-empirical models. For each method, the mean unsigned error (MUE) and cumulative probability percentiles, Q_n ($n = 50, 75, 90$, and 95) are reported in log-scale. Methods are sorted in ascending order of MUE. Values in square brackets are the Spearman rank correlations w.r.t experimental values. Vertical lines on the percentile points denote the standard deviation estimated via bootstrapping.

normalized) error consist of either several atoms or several electrons. The hydrocarbons cycloheptadecane and 9,10-diphenylanthracene show the largest extensive error; from opposite signs of the errors of these two compounds, one may speculate that the source of their errors cannot be due to the uncertainties associated with the parameters used in the enthalpy evaluation (see Section VID for a discussion).

It is important to compare the accuracy of the G4(MP2) and ccCA results presented above, based on the present implementation, to that of legacy implementations of these cWFTs. Firstly, all our calculations are based on a framework employing spherical primitive Gaussian type orbitals (GTOs), while Pople basis sets—used for B3LYP geometry relaxation, and G4(MP2) energies—are conventionally used in the Cartesian primitive GTO framework. Secondly, the ccCA-P³⁸ formalism uses B3LYP/cc-pVTZ reference geometry with Hartree-Fock and MP2 energies extrapolated separately to the CBS limit, relativistic DKH2 corrections for open-shell molecules calculated with a spin-collinear (*i.e.* UHF) reference wavefunction, and employs a different scale factor for ZPVE. To this end, in Table II, we compare prediction errors in our cWFT calculations for the entire G3/05 dataset to that of previously published results with same methods. For comparison, we have also summarized previous results based on the more accurate G4 theory.

As far as the G4(MP2) results are concerned, going from Cartesian GTOs to spherical GTOs leads to a tiny increase in the MUE by 0.01 kcal/mol. Our prediction error for ccCA fares rather well when com-

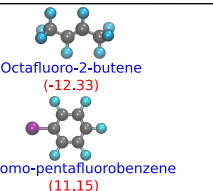

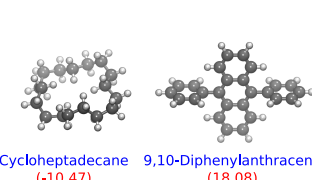
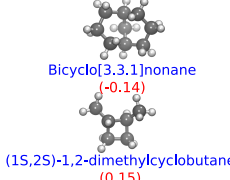
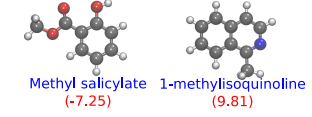
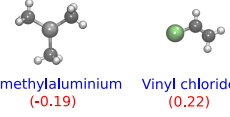


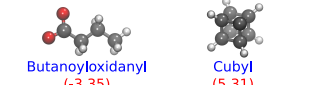
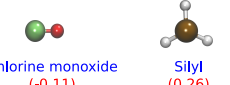
	Error	Error per Valence Electron
Non-Hydrogens	 <p>Octafluoro-2-butene (-12.33)</p> <p>1-Bromo-pentafluorobenzene (11.15)</p>	 <p>Dilithium (-0.74)</p> <p>Calcium Oxide (0.37)</p>
Hydrocarbons	 <p>Cycloheptadecane (-10.47)</p> <p>9,10-Diphenylanthracene (18.08)</p> <p>Bicyclo[3.3.1]nonane (-0.14)</p>	 <p>(15,25)-1,2-dimethylcyclobutane (0.15)</p>
Subst. Hydrocarbons	 <p>Methyl salicylate (-7.25)</p> <p>1-methylisoquinoline (9.81)</p>	 <p>Trimethylaluminium (-0.19)</p> <p>Vinyl chloride (0.22)</p>
Inorganic hydrides	 <p>Dihydrogen sulfate (-4.15)</p> <p>Disilane (1.96)</p>	 <p>Hydroxylamine (-0.16)</p> <p>Silylene (0.26)</p>
Radicals	 <p>Butanoyloxidanyl (-3.35)</p> <p>Cubyl (5.31)</p>	 <p>Chlorine monoxide (-0.11)</p> <p>Silyl (0.26)</p>

FIG. 7. Left column presents molecules in the PPE1694 dataset exhibiting the highest deviations in G4(MP2) predicted ΔH_f° . Right column shows molecules with extreme errors per valence electron.

pared to ccCA-P values from Ref. 38, while the original formalism—with a larger basis set for geometry optimization—showing much smaller error for the binding energy of hydrogen bonded dimers. While we believe that the accuracy of our ccCA results can improve when adopting the ccCA settings to be similar to that of the ccCA-P³⁸ implementation, here we used settings that render a comparison between G4(MP2) and ccCA seamless.

Further, we have extended the comparison between cWFTs to the slightly larger dataset – Pedley CHONF (see Section III); we note our G4(MP2) results to agree fairly well with that of previously reported values from Ref. 5. Interestingly, for G4 and G4(MP2) we find the accuracies for hydrocarbons and their substituted analogues to be retained when going from the G3/05 set to Pedley CHONF. As for ccCA, the MUE of 1.01 kcal/mol for the Pedley CHONF dataset is comparable to that of the total error for the G3/05 set, indicating the small deviations in both values to lie within the uncertainties in the reference experimental values.

TABLE II. Comparison between errors in G4(MP2), ccCA and G4 for G3/05 and Pedley CHONF. Both results from previous and current studies are included for all classes of compounds.

Dataset	G4(MP2)	ccCA	G4
A. G3/05 (452) ^a	1.05, 1.04 ^b	0.98, 0.99 ^c	0.83 ^d
1. ΔH_f° (270)	1.00, 0.99 ^b	0.93, 0.95 ^c	0.80 ^d
-Nonhydrogens (79)	1.46, 1.44 ^b	1.04	1.13 ^d
-Hydrocarbons (38)	0.64, 0.63 ^b	0.96	0.48 ^d
-Subst. Hydrocarbons (100)	0.84, 0.83 ^b	0.85	0.68 ^d
-Inorganic hydrides (19)	0.92, 0.94 ^b	0.99	0.92 ^d
-Radicals (34)	0.83, 0.86 ^b	0.82	0.66 ^d
2. IP (103) ^a	1.08, 1.07 ^b	1.08, 1.09 ^c	0.91 ^d
-Atoms (26)	1.12, 1.13 ^b	0.55	0.65 ^d
-Molecules (77)	1.06, 1.05 ^b	1.26	0.99 ^d
3. EA (63)	1.26, 1.23 ^b	0.97, 1.03 ^c	0.83 ^d
-Atoms (14)	1.86, 1.84 ^b	0.89	0.91 ^d
-Molecules (49)	1.10, 1.06 ^b	1.00	0.81 ^d
4. PA (10)	0.66, 0.67 ^b	1.23, 0.93 ^c	0.84 ^d
5. BE (6)	1.29, 1.28 ^b	1.15, 0.58 ^c	1.12 ^d
B. Pedley CHONF, ΔH_f° (459)	0.76, 0.79 ^e	1.01	0.69
-Hydrocarbons (175)	0.61, 0.68 ^e	0.84	0.51
-Subst. hydrocarbons (284)	0.86, 0.86 ^e	1.12	0.80

^a We have excluded two triplet entries for H₂S and N₂

^b from Ref. 37

^c from Ref. 38

^d from Ref. 23

^e from Ref. 5

B. Transferability of HLC in G4(MP2)

An interesting point of concern in the G_n -series of cWFTs—more specifically G4(MP2)—is the role HLC plays in the model. The total G4(MP2) electronic energy takes the form

$$E_0^{G4(MP2)} = E_{GTBAS1}^{CCSD(T)} + \Delta E^{MP2} + \Delta E^{HF} + \text{ZPVE} + \text{SO} + \text{HLC} \quad (8)$$

The HLC term, as pointed out by Martin^{21,106–109}, accounts for the residual error introduced in the additive model when there is significant coupling between the one-particle basis set and N -electron correlated wavefunction. However, it is long known that the success of the HLC correction in G_n methods is strongly coupled to the choice of basis sets employed. To quote John Pople¹¹⁰—from the first study on the G1 method—“Uniform application of the HLC is only sensible if the basis used, 6–311+G** (2df), is reasonably balanced, meaning that residual errors per electron are approximately constant over a wide range of molecules.”. HLC has been modified over the years through G1¹¹⁰, G2¹¹¹, G3¹¹² and G4²³ studies. In G4(MP2)³⁷, the HLC terms take the same form as in

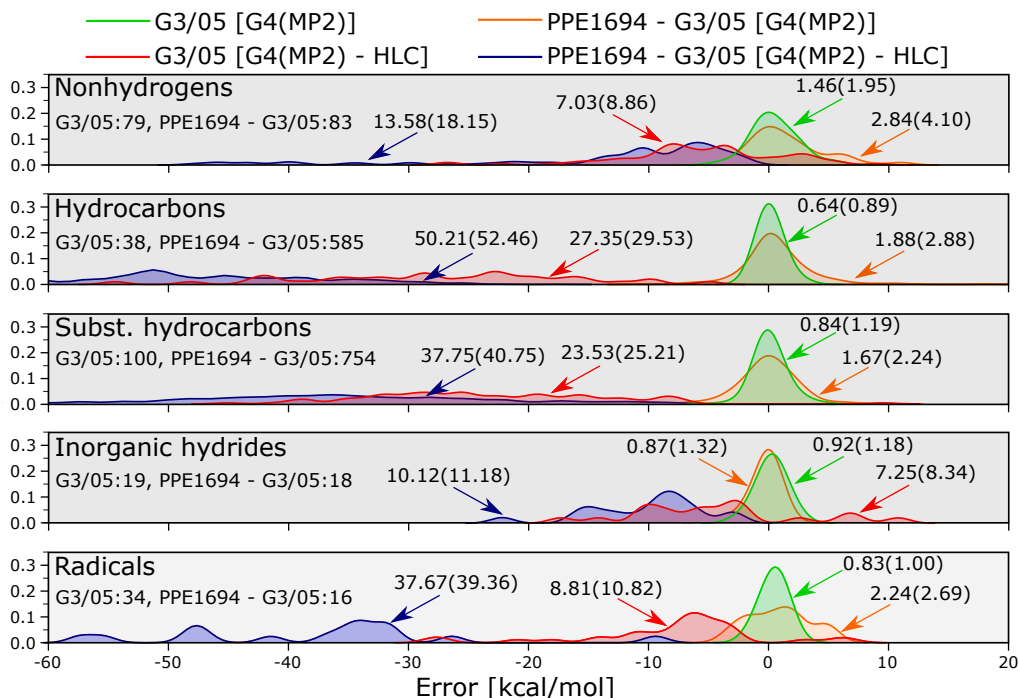


FIG. 8. Influence of HLC in determining ΔH_f° for various classes of compounds in the G3/05 dataset and rest of the compounds in the PPE1694 dataset. For both sets, results are shown separately with and without the HLC term. The arrows point to MUE (RMSE) for each error distribution. The lower bound of the error is set to -60 kcal/mol for clarity.

G4 but with parameters optimized separately:

$$\text{HLC}^{\text{G4(MP2)}} = \begin{cases} -An_\beta \\ -A'n_\beta - B(n_\alpha - n_\beta) \\ -Cn_\beta - D(n_\alpha - n_\beta) \\ -E \end{cases} \quad (9)$$

where the terms bear the same meaning as in the original G4 study²³.

In Fig. 8 we inspect the transferability of HLC across various classes of compounds in G3/05 and PPE1694. For nonhydrogens, HLC reduces the MUE \approx 5-times for both G3/05 and the remaining nonhydrogens in PPE1694. G3/05 hydrocarbons show a 43-fold decay in MUE without the HLC correction while the decay is 27-fold for the remaining ones in PPE1694. Drop in MUE is 28- and 23-fold for substituted hydrocarbons in G3/05 and the rest in PPE1694, respectively. For inorganic hydrides, MUE drops 8-fold for G3/05, while it is 12-fold for others in PPE1694. Radicals show a 11-fold decay in MUE for G3/05 while the rest in PPE1694 show a 17-fold drop. Though HLC captures systematic and non-systematic effects successfully across compound types and datasets, we do note the quantitative prediction accuracy of G4(MP2) to drop from 1.00 kcal/mol to 1.70 kcal/mol, when going from G3/05 (Table II) to PPE1694 (Table I). This drop in accuracy when increasing the dataset size may be ascribed to both the residual uncertainties in the experimental results, and also the system-

atic errors introduced in the form of empirical reference data for atoms, a topic that forms the subject of Section VID.

C. ISO32 dataset for isomerization reaction energies

Accurate prediction of isomerization energies is one of the stringent tests for testing the reliability of WFTs, cWFTs and DFAs¹¹³, since isomerization reaction energetics encode information about orbital hybridization, electronic conjugation, and steric effects in chemical bonding^{114,115}. Previous studies have observed several semi-local and hybrid DFAs to predict qualitatively incorrect trends for the energy ordering of constitutional isomers belonging for certain stoichiometries¹¹⁶. From the point of view of thermochemical procedures, all systematic contributions to molecular enthalpies such as empirical atomic corrections, and HLC are cancelled in isomerization energies. Hence, prediction errors expose non-systematic errors encoded in the evaluation of electronic energies. To arrive at a large benchmark suite of isomerization energies, we collected constitutional isomers belonging to 32 unique stoichiometries (we denote the set ISO32). All stoichiometries in the ISO32 dataset contains more than 7 constitutional isomers—for isomers with same $\Delta H_f^{\circ, \text{exp}}$, the system with lowest $\Delta H_f^{\circ, \text{G4(MP2)}}$ was considered—amounting to 517 unique

TABLE III. Accuracies of G4, G4(MP2), ccCA, CBS-QB3, ω B97M-D3BJ and ω B97M-V for the prediction of isomerization enthalpies for 32 sets of constitutional isomers: MUE is mean unsigned error (in kcal/mol), RMSE is root-mean-square-error (in kcal/mol), and ρ is the Spearman rank correlation coefficient; the latter quantity is reported per stoichiometry.

Stoichiometry (#)	MUE (RMSE, ρ)					
	G4	G4(MP2)	ccCA	CBS-QB3	ω B97M-D3BJ	ω B97M-V
C ₄ H ₆ (7)	0.91 (1.13, 0.98)	1.03 (1.18, 0.98)	0.80 (1.02, 1.00)	0.96 (1.21, 0.98)	1.50 (2.12, 0.98)	2.19 (2.68, 1.00)
C ₅ H ₈ (12)	0.81 (0.89, 0.99)	0.85 (0.94, 0.98)	0.40 (0.60, 0.99)	0.51 (0.61, 0.99)	1.02 (1.22, 0.98)	1.34 (1.56, 0.98)
C ₅ H ₁₀ (11)	0.79 (0.86, 0.99)	0.86 (0.90, 0.99)	0.26 (0.37, 0.99)	0.52 (0.64, 0.99)	0.42 (0.58, 0.99)	0.88 (0.90, 0.99)
C ₆ H ₈ (8)	1.11 (1.18, 0.98)	1.14 (1.24, 0.98)	0.89 (1.03, 1.00)	1.05 (1.13, 0.98)	0.72 (0.81, 1.00)	1.10 (1.23, 1.00)
C ₆ H ₁₀ (26)	0.96 (1.47, 0.99)	1.02 (1.54, 0.99)	0.91 (1.35, 0.99)	0.92 (1.38, 0.99)	1.15 (1.45, 0.99)	1.42 (1.70, 0.98)
C ₆ H ₁₂ (26)	0.87 (1.59, 0.97)	0.88 (1.55, 0.96)	0.84 (1.43, 0.97)	0.84 (1.45, 0.97)	1.02 (1.61, 0.97)	1.57 (1.93, 0.97)
C ₇ H ₈ (9)	1.79 (2.01, 0.96)	1.64 (1.96, 0.96)	1.63 (1.88, 0.96)	0.94 (1.20, 0.96)	1.30 (1.46, 0.96)	2.21 (2.63, 0.96)
C ₇ H ₁₂ (31)	1.18 (1.50, 0.97)	1.30 (1.64, 0.97)	1.38 (1.68, 0.97)	1.48 (1.74, 0.97)	1.36 (1.68, 0.98)	1.95 (2.37, 0.98)
C ₇ H ₁₄ (39)	0.66 (0.86, 0.91)	0.70 (0.94, 0.91)	0.60 (0.77, 0.93)	0.65 (0.83, 0.92)	0.49 (0.66, 0.94)	0.93 (1.12, 0.94)
C ₇ H ₁₆ (8)	0.37 (0.62, 0.97)	0.37 (0.62, 0.98)	0.47 (0.62, 0.97)	0.38 (0.61, 0.97)	0.62 (0.77, 0.95)	0.57 (0.69, 0.95)
C ₈ H ₁₀ (15)	1.43 (1.73, 0.98)	1.41 (1.78, 0.98)	1.34 (1.64, 0.98)	1.33 (1.60, 0.98)	1.13 (1.46, 0.99)	1.71 (2.11, 0.99)
C ₈ H ₁₄ (14)	1.14 (2.25, 0.94)	1.18 (2.28, 0.95)	1.07 (2.19, 0.93)	1.10 (2.13, 0.94)	1.17 (2.24, 0.94)	1.29 (2.10, 0.94)
C ₈ H ₁₆ (77)	4.81 (4.98, 0.89)	5.04 (5.21, 0.88)	4.60 (4.76, 0.89)	4.54 (4.73, 0.89)	4.87 (5.01, 0.89)	3.99 (4.19, 0.89)
C ₈ H ₁₈ (17)	1.77 (2.17, 0.69)	1.83 (2.22, 0.69)	1.23 (1.60, 0.59)	1.56 (1.98, 0.72)	1.24 (1.38, 0.53)	1.21 (1.37, 0.56)
C ₉ H ₁₀ (7)	0.66 (0.80, 0.86)	0.75 (0.89, 0.86)	0.82 (0.94, 0.76)	0.90 (1.13, 0.93)	0.82 (0.86, 0.76)	1.50 (1.66, 0.76)
C ₉ H ₁₂ (13)	0.82 (1.04, 0.99)	1.20 (1.68, 0.99)	1.11 (1.41, 0.99)	1.15 (1.50, 1.00)	0.89 (0.99, 0.99)	0.72 (1.07, 0.99)
C ₉ H ₁₆ (9)	2.91 (3.63, 0.93)	2.96 (3.71, 0.93)	2.42 (3.57, 0.96)	2.89 (3.56, 0.94)	2.39 (3.43, 0.95)	2.42 (3.23, 0.95)
C ₉ H ₁₈ (11)	3.62 (3.91, 0.71)	3.59 (3.90, 0.71)	3.43 (3.78, 0.62)	3.55 (3.85, 0.71)	2.95 (3.38, 0.72)	3.07 (3.45, 0.73)
C ₁₀ H ₁₀ (10)	5.35 (5.91, 1.00)	5.51 (6.21, 1.00)	5.66 (6.17, 1.00)	5.97 (6.63, 1.00)	6.26 (6.93, 1.00)	6.44 (7.22, 1.00)
C ₁₀ H ₁₆ (9)	2.61 (3.14, 0.99)	2.32 (2.89, 0.99)	2.81 (3.15, 0.99)	3.01 (3.49, 0.99)	2.27 (2.60, 0.99)	3.34 (3.67, 0.99)
C ₇ H ₉ N(13)	1.08 (1.70, 0.99)	1.10 (1.98, 0.99)	1.23 (2.02, 0.98)	1.32 (2.14, 0.99)	1.38 (2.52, 0.99)	1.30 (2.43, 0.99)
C ₅ H ₁₀ O(11)	0.50 (0.64, 0.99)	0.45 (0.56, 0.99)	0.56 (0.71, 0.98)	0.71 (0.97, 0.97)	0.86 (0.94, 0.97)	0.75 (0.94, 0.97)
C ₅ H ₁₂ O(11)	0.64 (1.18, 0.93)	0.66 (1.24, 0.91)	0.68 (1.20, 0.93)	0.74 (1.21, 0.93)	0.85 (1.23, 0.95)	0.75 (1.16, 0.92)
C ₆ H ₁₂ O(7)	0.71 (0.75, 0.90)	0.60 (0.68, 0.93)	0.76 (0.90, 0.86)	0.84 (0.92, 0.90)	0.57 (0.74, 0.90)	0.90 (1.13, 0.86)
C ₆ H ₁₄ O(7)	0.73 (0.80, 0.83)	0.69 (0.76, 0.95)	0.84 (0.91, 0.98)	0.71 (0.86, 0.81)	0.60 (0.74, 0.95)	0.57 (0.76, 0.95)
C ₈ H ₁₀ O(12)	1.37 (1.60, 0.94)	1.37 (1.59, 0.94)	1.49 (1.69, 0.92)	1.38 (1.62, 0.92)	1.61 (1.85, 0.90)	1.56 (1.82, 0.92)
C ₄ H ₈ O ₂ (9)	1.49 (1.76, 1.00)	1.43 (1.64, 1.00)	1.40 (1.57, 1.00)	1.92 (2.25, 1.00)	1.15 (1.53, 1.00)	1.65 (1.89, 1.00)
C ₄ H ₁₀ O ₂ (8)	2.68 (2.88, 1.00)	2.60 (2.76, 1.00)	2.30 (2.47, 1.00)	2.84 (3.16, 1.00)	2.82 (2.96, 1.00)	2.88 (3.06, 1.00)
C ₅ H ₁₀ O ₂ (15)	3.09 (3.45, 0.98)	2.78 (3.14, 0.98)	2.68 (3.05, 0.98)	3.71 (4.13, 0.98)	2.31 (2.57, 0.98)	2.99 (3.41, 0.98)
C ₆ H ₁₂ O ₂ (16)	2.07 (2.79, 0.95)	2.28 (2.96, 0.95)	2.70 (3.36, 0.95)	1.82 (2.65, 0.95)	3.31 (3.89, 0.94)	2.53 (3.24, 0.94)
C ₅ H ₁₂ S(9)	0.61 (0.70, 0.87)	0.64 (0.78, 0.88)	0.45 (0.64, 0.88)	0.67 (0.78, 0.89)	0.64 (0.79, 0.83)	0.53 (0.68, 0.83)
C ₆ H ₁₄ S(8)	1.29 (1.83, 0.87)	1.31 (1.85, 0.87)	0.87 (1.57, 0.78)	1.25 (1.79, 0.85)	0.96 (1.53, 0.82)	0.85 (1.48, 0.80)
Total(485)	1.94 (2.75)	2.00 (2.85)	1.86 (2.67)	1.94 (2.75)	1.96 (2.79)	2.04 (2.72)

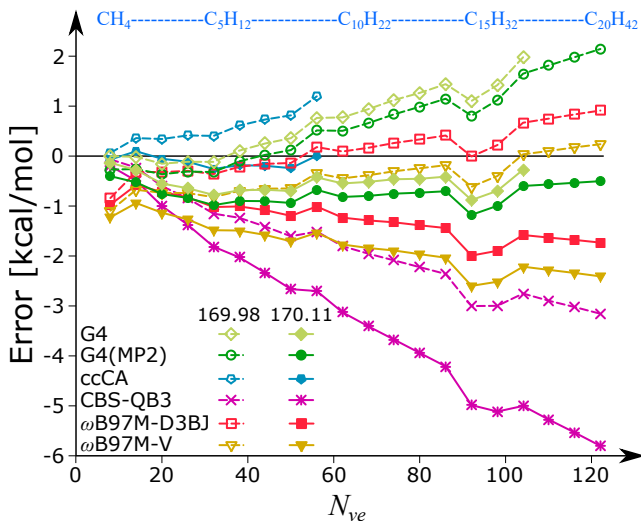
systems.

Table III presents mean errors in the prediction of isomerization energies where the reactant is the global minimum per stoichiometry, amounting to 485 reaction energies. Due to the computational complexity, we could not perform ccCA calculations for 5 molecules: C₈H₁₄ (1), C₉H₁₆ (3) and C₉H₁₈ (1). The accuracies of cWFTs are found to be better than DFTs', with ccCA providing the smallest MUE of 1.86 kcal/mol and ω B97M-V showing the largest MUE, 2.04 kcal/mol. Interestingly, CBS-QB3 shows a similar prediction accuracy to G4; G4(MP2) accuracy falling shortly behind. Benchmarking of isomerization energies benefits greatly through a joint analysis of MUE and the Spearman rank correlation (ρ). For instance, all methods show large MUEs for the isomers of C₁₀H₁₀, albeit scoring a perfect $\rho = 1.0$ suggesting the presence of a systematic shift in the calculated results. In contrary, the isomers of C₈H₁₈ presents a small MUE but their ρ scores poorly, reaching as low as 0.53, suggesting the isomers to be ther-

modynamically competitive. Overall, when averaging over all 485 reaction energies, we find the error trend ccCA < G4 \approx CBS-QB3 < ω B97M-D3BJ < G4(MP2) < ω B97M-V (see Table III) In Table IV, we present the error metrics only for the global minima in ISO32. While both DFAs deliver similar average errors, one notes their stoichiometry-specific errors to be somewhat inconsistent. The general error in the modeling of global minima across stoichiometries follows G4 < ω B97M-V < ccCA \approx ω B97M-D3BJ < G4(MP2) < CBS-QB3 agreeing with the deep-rooted view: G4 is a better thermochemistry model than ccCA. As stated above, ccCA's performance can be improved by extending the size of the basis sets utilized, which however may restrict the method's applicability to large systems.

TABLE IV. Accuracies of methods in determining the ΔH_f° of global minimum of each stoichiometry in ISO32****

#	Global minimum (Stoichiometry)	$\Delta H_f^{\circ, \text{calc.}} (\Delta H_f^{\circ, \text{exp.}} - \Delta H_f^{\circ, \text{calc.}})$						
		G4	G4(MP2)	ccCA	CBS-QB3	ω B97M-D3BJ	ω B97M-V	
1	1,3-Butadiene (C ₄ H ₆)	26.23	26.52 (-0.29)	25.72 (0.51)	27.21 (-0.98)	28.27 (-2.04)	27.42 (-1.19)	28.24 (-2.01)
2	Cyclopentene (C ₅ H ₈)	7.91	8.94 (-1.03)	8.44 (-0.53)	8.92 (-1.01)	10.35 (-2.44)	8.63 (-0.72)	8.50 (-0.59)
3	Cyclopentane (C ₅ H ₁₀)	-18.28	-17.39 (-0.89)	-17.36 (-0.92)	-17.87 (-0.41)	-17.00 (-1.28)	-17.73 (-0.55)	-18.00 (-0.28)
4	Methylcyclopentadiene (C ₆ H ₈)	23.90	23.68 (0.22)	22.88 (1.02)	24.63 (-0.73)	25.96 (-2.06)	23.94 (-0.04)	23.80 (0.10)
5	Cyclohexene (C ₆ H ₁₀)	-1.15	-0.66 (-0.49)	-1.14 (-0.01)	-0.38 (-0.77)	1.14 (-2.29)	-0.78 (-0.37)	-0.84 (-0.31)
6	Cyclohexane (C ₆ H ₁₂)	-29.49	-28.89 (-0.60)	-28.86 (-0.63)	-28.99 (-0.50)	-27.50 (-1.99)	-28.73 (-0.76)	-28.97 (-0.52)
7	Toluene (C ₇ H ₈)	12.00	11.98 (0.02)	11.02 (0.98)	13.59 (-1.59)	13.60 (-1.60)	11.35 (0.65)	11.62 (0.38)
8	Bicyclo[2.2.1]heptane (C ₇ H ₁₂)	-12.96	-13.47 (0.51)	-13.58 (0.62)	-12.87 (-0.09)	-11.91 (-1.05)	-12.30 (-0.66)	-13.69 (0.73)
9	Methylcyclohexane (C ₇ H ₁₄)	-36.98	-36.64 (-0.34)	-36.60 (-0.38)	-36.44 (-0.54)	-34.85 (-2.13)	-35.85 (-1.13)	-36.21 (-0.77)
10	2,2-Dimethylpentane (C ₇ H ₁₆)	-49.20	-49.27 (0.07)	-49.11 (-0.09)	-49.00 (-0.20)	-47.49 (-1.71)	-47.46 (-1.74)	-47.23 (-1.97)
11	1,3-Dimethylbenzene (C ₈ H ₁₀)	4.12	4.05 (0.07)	3.24 (0.88)	6.13 (-2.01)	6.05 (-1.93)	3.92 (0.20)	4.12 (-0.00)
12	Bicyclo[2.2.2]octane (C ₈ H ₁₄)	-23.66	-22.78 (-0.88)	-22.81 (-0.85)	-21.98 (-1.68)	-20.74 (-2.92)	-21.61 (-2.05)	-22.95 (-0.71)
13	(1R,2R,3S)-1,2,3-trimethylcyclopentane (C ₈ H ₁₆)	-45.09	-40.20 (-4.89)	-40.09 (-5.00)	-39.59 (-5.50)	-37.99 (-7.10)	-38.66 (-6.43)	-39.24 (-5.85)
14	2,2,3,3-Tetramethylbutane (C ₈ H ₁₈)	-53.92	-55.01 (1.09)	-54.92 (1.00)	-53.82 (-0.10)	-52.74 (-1.18)	-51.57 (-2.35)	-51.53 (-2.39)
15	2,3-Dihydro-1H-indene (C ₉ H ₁₀)	14.51	13.90 (0.61)	12.96 (1.55)	16.21 (-1.70)	15.82 (-1.31)	13.63 (0.88)	13.05 (1.46)
16	1,3,5-Trimethylbenzene (C ₉ H ₁₂)	-3.80	-3.92 (0.12)	-4.58 (0.78)	-1.41 (-2.39)	-1.41 (-2.39)	-3.56 (-0.24)	-3.44 (-0.36)
17	trans-Octahydro-1H-indene (C ₉ H ₁₆)	-31.43	-31.48 (0.05)	-31.51 (0.08)	-30.67 (-0.76)	-29.01 (-2.42)	-30.26 (-1.17)	-31.49 (0.06)
18	(1a,3a,5a)-1,3,5-Trimethylcyclohexane (C ₉ H ₁₈)	-50.69	-52.19 (1.50)	-52.10 (1.41)	-51.27 (0.58)	-49.55 (-1.14)	-49.98 (-0.71)	-50.58 (-0.11)
19	2-Methylindene (C ₁₀ H ₁₀)	33.15	28.61 (4.54)	27.31 (5.84)	31.79 (1.36)	31.38 (1.77)	29.09 (4.06)	28.53 (4.62)
20	Adamantane (C ₁₀ H ₁₆)	-31.90	-33.90 (2.00)	-33.90 (2.00)	-31.58 (-0.32)	-30.87 (-1.03)	-30.66 (-1.24)	-33.07 (1.17)
21	2-Methylaniline (C ₇ H ₉ N)	12.72	12.37 (0.35)	11.74 (0.98)	13.73 (-1.01)	13.94 (-1.22)	11.42 (1.30)	11.26 (1.46)
22	3-Methyl-2-butanone (C ₅ H ₁₀ O)	-62.75	-62.77 (0.02)	-62.32 (-0.43)	-62.53 (-0.22)	-62.55 (-0.20)	-63.75 (1.00)	-63.41 (0.66)
23	2-Methyl-2-butanol (C ₅ H ₁₂ O)	-79.06	-79.32 (0.26)	-78.76 (-0.30)	-79.59 (0.53)	-79.29 (0.23)	-78.62 (-0.44)	-78.87 (-0.19)
24	3-3-Dimethyl-2-butanone (C ₆ H ₁₂ O)	-69.47	-70.09 (0.62)	-69.63 (0.16)	-69.34 (-0.13)	-69.56 (0.09)	-70.13 (0.66)	-69.92 (0.45)
25	3-Hexanol (C ₆ H ₁₄ O)	-79.30	-80.18 (0.88)	-79.66 (0.36)	-80.85 (1.55)	-79.90 (0.60)	-80.09 (0.79)	-80.19 (0.89)
26	2,4-Dimethylphenol (C ₈ H ₁₀ O)	-38.93	-38.12 (-0.81)	-38.58 (-0.35)	-36.27 (-2.66)	-37.46 (-1.47)	-39.14 (0.21)	-39.40 (0.47)
27	2-Methylpropanoic-acid (C ₄ H ₈ O ₂)	-115.70	-114.12 (-1.58)	-113.46 (-2.24)	-114.35 (-1.35)	-115.21 (-0.49)	-116.19 (0.49)	-116.21 (0.51)
28	(2R,3S)-2,3-butanediol (C ₄ H ₁₀ O ₂)	-114.64	-111.32 (-3.32)	-110.53 (-4.11)	-112.27 (-2.37)	-112.73 (-1.91)	-111.81 (-2.83)	-112.36 (-2.28)
29	3-Methylbutanoic acid (C ₅ H ₁₀ O ₂)	-122.45	-119.99 (-2.46)	-119.37 (-3.08)	-120.26 (-2.19)	-120.79 (-1.66)	-122.19 (-0.26)	-122.16 (-0.29)
30	Hexanoic acid (C ₆ H ₁₂ O ₂)	-122.35	-123.13 (0.78)	-122.48 (0.13)	-123.63 (1.28)	-123.63 (1.28)	-125.74 (3.39)	-125.55 (3.20)
31	2,2-Dimethyl-1-propanethiol (C ₅ H ₁₂ S)	-30.83	-31.78 (0.95)	-32.68 (1.85)	-31.90 (1.07)	-31.83 (1.00)	-30.88 (0.05)	-30.84 (0.01)
32	2-Methyl-2-pentanethiol (C ₆ H ₁₄ S)	-35.44	-36.89 (1.45)	-37.60 (2.16)	-36.67 (1.23)	-36.44 (1.00)	-35.31 (-0.13)	-35.39 (-0.05)
MUE			1.05	1.29	1.21	1.65	1.21	1.09

FIG. 9. Systematic errors in G4, G4(MP2), ccCA, CBS-QB3, ω B97M-D3BJ and ω B97M-V predictions of ΔH_f° due to the choice of $\Delta H_f^\circ(C_{\text{gas}}, 0 \text{ K})$ shown for the smallest 20 linear alkanes.

D. Source of Systematic Errors in Formation Enthalpies

Molecular $\Delta H_f^\circ(298 \text{ K})$ depends on enthalpies of constituent atoms in their standard elemental forms. The absolute enthalpies per atom for the elements enter the calculation as empirical constants: $\Delta H_f^\circ(0 \text{ K})$, which is the zero-Kelvin enthalpy of formation; and the associated thermal correction, $H^\circ(298 \text{ K}) - H^\circ(0 \text{ K})$. The former quantity contributes predominantly to the total enthalpy, hence any uncertainty in its determination will be accrued with increasing molecular size. This has been exemplified by Tasi *et al.*,¹¹⁷ for C₁-C₁₃ alkanes modelled with G2(MP2,SVP), where large systematic errors were noted when the conventional value of $\Delta H_f^\circ(0 \text{ K})=169.98$ kcal/mol was used for the C atom. A re-evaluated value of 170.11 kcal/mol was shown to reduce systematic errors for that dataset.

We have revisited the case of linear alkanes by increasing the set until icosane (C₂₀H₄₂) and modeling ΔH_f° with the four cWFTs along with ω B97M-D3BJ and ω B97M-V DFAs. Fig. 9 displays the prediction errors for all 6 methods employing two values of $\Delta H_f^\circ(C_{\text{gas}}, 0 \text{ K})$: 169.98 kcal/mol and 170.11 kcal/mol. We find all cWFTs except CBS-QB3 to benefit from the systematic shift resulting in reduced prediction errors—ccCA agreeing with the experimental values for C₁-C₉ alkanes better

than G4 and G4(MP2). The DFA, ω B97M-D3BJ which showed excellent agreement with experimental values of ΔH_f° with an MUE of 0.37 kcal/mol, when using the conventional $\Delta H_f^\circ(C_{\text{gas}}, 0 \text{ K})$ deteriorates to 1.29 kcal/mol upon using the re-evaluated parameter. Similarly ω B97M-V's mean error rises from 0.48 kcal/mol to 1.82 kcal/mol when switching from $\Delta H_f^\circ(C_{\text{gas}}, 0 \text{ K}) = 169.98 \text{ kcal/mol}$ to $\Delta H_f^\circ(C_{\text{gas}}, 0 \text{ K}) = 170.11 \text{ kcal/mol}$.

VII. CONCLUSIONS

A benchmark dataset of experimental ΔH_f° for 1,694 compounds that are electronically and structurally rich is presented. This dataset was assembled by collecting several previously reported benchmark suites including the 'legacy' dataset—G3/05 comprising 247 entries. The resulting set included 102 'outliers' with potentially non-negligible experimental uncertainties detected with a probabilistic approach. The procedure also takes into consideration, uncertainties associated with the reference theory, G4.

A more robust approach would be to consider more than one high-fidelity reference methods and make a joint-probabilistic model to prune the dataset. The only tunable parameter in this model is the threshold percentile used for selecting valid benchmarks; this value was set to the 95th percentile for the reference method G4. We adopted a bootstrapping strategy to estimate the variance in the model arising from sampling bias. Our final results are based on the lower bound for the error-threshold to mark an entry as outlier.

For the PPE1694 dataset, we have presented extensive benchmark results of formation enthalpies with 4 cWFTs, *i.e.*, G4, G4(MP2), ccCA and CBS-QB3 as well as with 23 DFAs. Conventional error metrics such as MUE have been reported along with probabilistic metrics such as Q50, Q75, Q90, and Q95, that provide information about the probability and cumulative densities of errors as suggested in other studies^{93,118}. When compared to pruned experimental values, among the methods considered in this study, G4 delivers the best performance with an MUE of 1.47 kcal/mol, followed by ccCA and G4(MP2) with MUEs of 1.66 kcal/mol and 1.70 kcal/mol respectively. CBS-QB3 method has MUE of 2.82 kcal/mol. The semi-empirical methods PM6 and PM7, as expected, result in rather accurate ΔH_f° with MUEs ≈ 4 kcal/mol. The most popular DFA, B3LYP exhibits a MUE of over 4 kcal/mol. However, its long-range and dispersion corrected versions, namely, CAM-B3LYP and B3LYP-D3 exhibit MUEs ≈ 3 kcal/mol, while the GGA method BLYP, mGGA method TPSS, and the hybrid method X3LYP have MUEs in the 4 – 7 kcal/mol window. Dispersion corrected double hybrid functionals B2PLYP-D3 and mPW2PLYP-D show better performances with overall MUEs in 2 – 3 kcal/mol

range. For the prediction of ΔH_f° , we found the best performing class of DFAs to be the range-separated method ω B97X, and its modifications yielding rather accurate predictions with MUE ≈ 2 kcal/mol. As a general trend, we note empirical dispersion corrections to improve prediction accuracy.

Our analyses revealed that the original G4(MP2) method and the empirical parameterization of the HLC involved in that model retain their transferability going from the G3/05 set with 270 entries to the proposed PPE1694 set that is 6 times larger. This suggests that the prediction accuracy of G4(MP2) to hold not only for closed-shell, organic molecules of the type encountered in the QM9 dataset,^{5,30} but fairly well to datasets with free-radicals, non-hydrogens and inorganic hydrides. It will be compelling to see if modern functionals can be designed by benchmarking on the diverse dataset presented here. Similarly, it will be of interest to see if cWFTs based on additional parameterization such as in the G4(MP2)-6X method¹¹⁹ and its variants^{120,121} preserve their transferability going from the small molecules set to the PPE1694 set.

Further, from the entire benchmark suite presented here, we identified 32 sets of constitutional isomers; reaction enthalpies for this ISO32 dataset were benchmarked over G4, G4(MP2), ccCA, CBS-QB3, and the two best performing DFAs. For the prediction of 485 reaction energies, ccCA performs the best with an MUE of 1.86 kcal/mol followed by G4 and G4(MP2) with MUEs 1.94 kcal/mol and 2.00 kcal/mol respectively. In this case, the DFAs ω B97M-D3BJ and ω B97M-V have also yielded excellent predictions with MUEs ≈ 2 kcal/mol. When extending the application of G4(MP2) method to molecules with large number of C atoms, we find the prediction accuracy to be sensitive to an empirical atomic parameter, which suggests that a careful evaluation of these parameters for all atom types is essential to prevent systematic accumulation of errors. Such calibration could be done with a high-fidelity method such as W4 or HEAT-456(Q). Preferably such an effort could be undertaken by pruning the total dataset and retaining only highly-precise experimental entries. Thermochemistry modeling done at such a rigor has been shown to be sensitive even to the effect anharmonicity has on molecular ZPVE^{122,123}, hence these effects must be incorporated with methods such as second-order vibrational perturbation theory (VPT2)^{124,125}.

VIII. ACKNOWLEDGEMENTS

SKD is grateful to TIFR Hyderabad for a junior research fellowship. This project was funded by intramural funds at TIFR Hyderabad from the Department of Atomic Energy (DAE). All calculations have been performed using the Helios computer cluster, which is an integral part of the MolDis Big Data facility, TIFR Hy-

derabad (<https://moldis.tifrh.res.in/>).

IX. DATA AVAILABILITY

The data that support the findings of this study are openly available in the MolDis repository, <http://moldis.tifrh.res.in/data/prunedHOF>. The same information may also be obtained from the authors through an email request.

APPENDIX: EMPIRICAL PARAMETERS

TABLE V. Heats of formation of atoms at 0 K, $\Delta H_f^\circ(0\text{ K})$, and enthalpy corrections, for elements in their standard states, $H^\circ(298\text{ K}) - H^\circ(0\text{ K})$. For H, Li, Be, B, C, N, O, F, Na, Mg, Al, Si, P, S and Cl, we used values from Ref. 126. For elements with multiple entries the most recent one, marked by bold font, is used. All values in kcal/mol.

Atom	$\Delta H_f^\circ(0\text{ K})$	$H^\circ(298\text{ K}) - H^\circ(0\text{ K})$
K	21.4830 ¹²⁷	1.6926 ¹²⁷
Ca	42.3850 ¹²⁷	1.3709 ¹²⁷
Ga	64.7633 ¹²⁷	1.3291 ¹²⁷
Br	28.1836 ¹²⁸	2.930 ^{128,129}
Ge	89.354 ¹³⁰ , 88.2 ¹³¹	1.104 ^{130,132}
As	68.86 ¹³³ , 68.8 ^{130,134}	1.23 ¹³²
Se	57.899 ¹³⁵	1.319 ¹³⁵

X. REFERENCES

- J. Cioslowski, *Quantum-mechanical prediction of thermochemical data* (Springer Science & Business Media, 2002).
- K. K. Irikura and D. J. Frurip, *Computational Thermochemistry* (ACS Publications, 1998) Chap. 1, pp. 2–18.
- O. A. von Lilienfeld, *Angew. Chem. Int. Ed.* **57**, 4164 (2018).
- R. Ramakrishnan and O. A. von Lilienfeld, *Rev. Comp. Ch.* **30**, 225 (2017).
- B. Narayanan, P. C. Redfern, R. S. Assary, and L. A. Curtiss, *Chem. Sci.* **10**, 7449 (2019).
- J. Hachmann, R. Olivares-Amaya, S. Atahan-Evrenk, C. Amador-Bedolla, R. S. Sánchez-Carrera, A. Gold-Parker, L. Vogt, A. M. Brockway, and A. Aspuru-Guzik, *J. Phys. Chem. Lett.* **2**, 2241 (2011).
- S. Chakraborty, P. Kayastha, and R. Ramakrishnan, *J. Chem. Phys.* **150**, 114106 (2019).
- J. Arús-Pous, M. Awale, D. Probst, and J.-L. Reymond, *CHIMIA* **73**, 1018 (2019).
- J. Aston, *Ind. Eng. Chem* **34**, 514 (1942).
- H. Duus, *Ind. Eng. Chem* **47**, 1445 (1955).
- A. S. Rodgers, *J. Phys. Chem.* **71**, 1996 (1967).
- O. V. Dorofeeva, V. P. Novikov, and D. B. Neumann, *J. Phys. Chem. Ref. Data* **30**, 475 (2001).
- L. A. Curtiss, P. C. Redfern, and D. J. Frurip, in *Reviews of Computational Chemistry*, Vol. 15, edited by K. B. Lipkowitz and D. B. Boyd (Wiley VCH, New York, 2000) pp. 147–211.
- L. A. Curtiss, P. C. Redfern, and K. Raghavachari, *WIREs Comput. Mol. Sci.* **1**, 810 (2011).
- F. Jensen, *Introduction to computational chemistry* (John Wiley & sons, 2017).
- A. Karton, *WIREs Comput. Mol. Sci.* **6**, 292 (2016).
- A. Karton, E. Rabinovich, J. M. Martin, and B. Ruscic, *J. Chem. Phys.* **125**, 144108 (2006).
- Y. J. Bomble, J. Vázquez, M. Kállay, C. Michauk, P. G. Szalay, A. G. Császár, J. Gauss, and J. F. Stanton, *J. Chem. Phys.* **125**, 064108 (2006).
- M. E. Harding, J. Vázquez, B. Ruscic, A. K. Wilson, J. Gauss, and J. F. Stanton, *J. Chem. Phys.* **128**, 114111 (2008).
- D. W. Rogers, *Heats of hydrogenation: experimental and computational hydrogen thermochemistry of organic compounds* (World Scientific: Long Island, NY, 2006).
- J. M. Martin, *Annu. Rep. Comput. Chem.* **1**, 31 (2005).
- J. Montgomery Jr, J. Ochterski, and G. Petersson, *J. Chem. Phys.* **101**, 5900 (1994).
- L. A. Curtiss, P. C. Redfern, and K. Raghavachari, *J. Chem. Phys.* **126**, 084108 (2007).
- N. J. DeYonker, T. R. Cundari, and A. K. Wilson, *J. Chem. Phys.* **124**, 114104 (2006).
- N. J. DeYonker, T. Grimes, S. Yockel, A. Dinescu, B. Mintz, T. R. Cundari, and A. K. Wilson, *J. Chem. Phys.* **125**, 104111 (2006).
- A. K. Wilson, N. J. DeYonker, and T. R. Cundari, in *Advances in the Theory of Atomic and Molecular Systems (Progress in Theoretical Chemistry and Physics)*, Vol. 19, edited by P. Piecuch, J. Maruani, G. Delgado-Barrio, and S. Wilson (Springer, Netherlands, 2009) pp. 197–224.
- L. Ruddigkeit, R. Van Deursen, L. C. Blum, and J.-L. Reymond, *J. Chem. Inf. Model.* **52**, 2864 (2012).
- F. A. Faber, A. S. Christensen, B. Huang, and O. A. von Lilienfeld, *J. Chem. Phys.* **148**, 241717 (2018).
- N. Lubbers, J. S. Smith, and K. Barros, *J. Chem. Phys.* **148**, 241715 (2018).
- R. Ramakrishnan, P. O. Dral, M. Rupp, and O. A. von Lilienfeld, *Sci. Data* **1**, 140022 (2014).
- R. Ramakrishnan, P. O. Dral, M. Rupp, and O. A. von Lilienfeld, *J. Chem. Theory Comput.* **11**, 2087 (2015).
- H. Kim, J. Y. Park, and S. Choi, *Sci. Data* **6**, 109 (2019).
- L. Ward, B. Blaiszik, I. Foster, R. S. Assary, B. Narayanan, and L. Curtiss, *MRS Commun.* **9**, 891 (2019).
- N. K. Dandu, L. Ward, R. S. Assary, P. C. Redfern, B. Narayanan, I. T. Foster, and L. A. Curtiss, *J. Phys. Chem. A* (2020), 10.1021/acs.jpca.0c01777.
- J. Pedley, R. D. Naylor, S. P. Kirby, et al., *Thermochemical data of organic compounds* (Chapman and Hall, 1986).
- J. Pedley, *Thermochemical data and structures of organic compounds*, Vol. 1 (CRC Press, 1994).
- L. A. Curtiss, P. C. Redfern, and K. Raghavachari, *J. Chem. Phys.* **127**, 124105 (2007).
- N. J. DeYonker, B. R. Wilson, A. W. Pierpont, T. R. Cundari, and A. K. Wilson, *Mol. Phys.* **107**, 1107 (2009).
- L. A. Curtiss, P. C. Redfern, and K. Raghavachari, *J. Chem. Phys.* **123**, 124107 (2005).
- M. Schwilk, D. N. Tahchieva, and O. A. von Lilienfeld, arXiv preprint arXiv:2004.10600 (2020).
- F. Neese, *WIREs Comput. Mol. Sci.* **2**, 73 (2012).
- F. Neese, *WIREs Comput. Mol. Sci.* **8**, e1327 (2018).
- N. J. DeYonker, T. G. Williams, A. E. Imel, T. R. Cundari, and A. K. Wilson, *J. Chem. Phys.* **131**, 024106 (2009).
- M. L. Laury, N. J. DeYonker, W. Jiang, and A. K. Wilson, *J. Chem. Phys.* **135**, 214103 (2011).
- C. Peterson, D. Penchoff, and A. Wilson, in *Annual Reports in Computational Chemistry*, Vol. 12 (Elsevier, 2016) pp. 3–45.
- M. J. Frisch, G. W. Trucks, H. B. Schlegel, G. E. Scuseria, M. A. Robb, J. R. Cheeseman, G. Scalmani, V. Barone, G. A. Petersson, H. Nakatsuji, X. Li, M. Caricato, A. V. Marenich, J. Bloino, B. G. Janesko, R. Gomperts, B. Mennucci, H. P. Hratchian, J. V. Ortiz, A. F. Izmaylov, J. L. Sonnenberg, D. Williams-Young, F. Ding, F. Lipparini, F. Egidi, J. Goings, B. Peng, A. Petrone, T. Henderson, D. Ranasinghe, V. G. Zakrzewski, J. Gao, N. Rega, G. Zheng, W. Liang,

- M. Hada, M. Ehara, K. Toyota, R. Fukuda, J. Hasegawa, M. Ishida, T. Nakajima, Y. Honda, O. Kitao, H. Nakai, T. Vreven, K. Throssell, J. A. Montgomery, Jr., J. E. Peralta, F. Ogliaro, M. J. Bearpark, J. J. Heyd, E. N. Brothers, K. N. Kudin, V. N. Staroverov, T. A. Keith, R. Kobayashi, J. Normand, K. Raghavachari, A. P. Rendell, J. C. Burant, S. S. Iyengar, J. Tomasi, M. Cossi, J. M. Millam, M. Klene, C. Adamo, R. Cammi, J. W. Ochterski, R. L. Martin, K. Morokuma, O. Farkas, J. B. Foresman, and D. J. Fox, "Gaussian¹⁶ Revision C.01," (2016), gaussian Inc. Wallingford CT.
- ⁴⁷J. J. Stewart, *J. Mol. Model.* **13**, 1173 (2007).
- ⁴⁸J. J. Stewart, *J. Mol. Model.* **19**, 1 (2013).
- ⁴⁹J. J. Stewart, "Mopac2016," (2016), Stewart Computational Chemistry, Colorado Springs, CO, USA, Available at <http://OpenMOPAC.net>.
- ⁵⁰J. P. Perdew and K. Schmidt, in *AIP Conference Proceedings*, Vol. 577 (American Institute of Physics, 2001) pp. 1–20.
- ⁵¹A. D. Becke, *Phys. Rev. A* **38**, 3098 (1988).
- ⁵²J. Perdew, J. Chevary, and S. Vosko, *Phys. Rev. B* **46**, 6671 (1992).
- ⁵³J. P. Perdew, K. Burke, and M. Ernzerhof, *Phys. Rev. Lett.* **78**, 1396 (1997).
- ⁵⁴A. D. Becke, *J. Chem. Phys.* **98**, 5648 (1993).
- ⁵⁵A. J. Cohen and N. C. Handy, *Mol. Phys.* **99**, 607 (2001).
- ⁵⁶X. Xu and W. A. Goddard, *Proc. Natl. Acad. Sci. USA* **101**, 2673 (2004).
- ⁵⁷C. Adamo and V. Barone, *J. Chem. Phys.* **110**, 6158 (1999).
- ⁵⁸J. Tao, J. P. Perdew, V. N. Staroverov, and G. E. Scuseria, *Phys. Rev. Lett.* **91**, 146401 (2003).
- ⁵⁹S. Grimme, *J. Phys. Chem. A* **109**, 3067 (2005).
- ⁶⁰Y. Zhao and D. G. Truhlar, *Theor. Chem. Acc.* **120**, 215 (2008).
- ⁶¹T. Yanai, D. P. Tew, and N. C. Handy, *Chem. Phys. Lett.* **393**, 51 (2004).
- ⁶²J.-D. Chai and M. Head-Gordon, *Phys. Chem. Chem. Phys.* **10**, 6615 (2008).
- ⁶³Y.-S. Lin, G.-D. Li, S.-P. Mao, and J.-D. Chai, *J. Chem. Theory Comput.* **9**, 263 (2013).
- ⁶⁴N. Mardirossian and M. Head-Gordon, *Phys. Chem. Chem. Phys.* **16**, 9904 (2014).
- ⁶⁵N. Mardirossian and M. Head-Gordon, *J. Chem. Phys.* **144**, 214110 (2016).
- ⁶⁶S. Grimme, S. Ehrlich, and L. Goerigk, *J. Comp. Chem.* **32**, 1456 (2011).
- ⁶⁷A. D. Becke and E. R. Johnson, *J. Chem. Phys.* **123**, 154101 (2005).
- ⁶⁸E. R. Johnson and A. D. Becke, *J. Chem. Phys.* **123**, 024101 (2005).
- ⁶⁹E. R. Johnson and A. D. Becke, *J. Chem. Phys.* **124**, 174104 (2006).
- ⁷⁰S. Grimme, *J. Chem. Phys.* **124**, 034108 (2006).
- ⁷¹S. Grimme, J. Antony, S. Ehrlich, and H. Krieg, *J. Chem. Phys.* **132**, 154104 (2010).
- ⁷²T. Schwabe and S. Grimme, *Phys. Chem. Chem. Phys.* **9**, 3397 (2007).
- ⁷³P. Linstrom and E. W.G. Mallard, "NIST chemistry webbook, NIST Standard Reference Database Number 69, National Institute of Standards and Technology, Gaithersburg MD, 20899," (2020), (Accessed December 2019).
- ⁷⁴H. E. Pence and A. Williams, "Chemspider: An online chemical information resource," (2010), (Accessed December 2019).
- ⁷⁵S. Kim, J. Chen, T. Cheng, A. Gindulyte, J. He, S. He, Q. Li, B. A. Shoemaker, P. A. Thiessen, B. Yu, *et al.*, *Nucleic Acids Res.* **47**, D1102 (2019).
- ⁷⁶M. D. Hanwell, D. E. Curtis, D. C. Lonie, T. Vandermeersch, E. Zurek, and G. R. Hutchison, *J. Cheminform* **4**, 17 (2012).
- ⁷⁷A. K. Rappé, C. J. Casewit, K. Colwell, W. A. Goddard III, and W. M. Skiff, *J. Am. Chem. Soc.* **114**, 10024 (1992).
- ⁷⁸F. Weigend and R. Ahlrichs, *Phys. Chem. Chem. Phys.* **7**, 3297 (2005).
- ⁷⁹J. W. Ochterski, *Thermochemistry in gaussian*, www.gaussian.com (2000), Accessed December 2019.
- ⁸⁰Note that in Table I of Ref. 82 SeH^+ has to be SeH .
- ⁸¹L. A. Curtiss, M. P. McGrath, J.-P. Blaudeau, N. E. Davis, R. C. Binning Jr, and L. Radom, *J. Chem. Phys.* **103**, 6104 (1995).
- ⁸²L. A. Curtiss, P. C. Redfern, V. Rassolov, G. Kedziora, and J. A. Pople, *J. Chem. Phys.* **114**, 9287 (2001).
- ⁸³M. M. Ghahremanpour, P. J. Van Maaren, and D. Van Der Spoel, *Sci. Data* **5**, 180062 (2018).
- ⁸⁴P. R. Schreiner, A. A. Fokin, R. A. Pascal, and A. de Meijere, *Org. Lett.* **8**, 3635 (2006).
- ⁸⁵A. Sengupta and K. Raghavachari, *J. Chem. Theory Comput.* **10**, 4342 (2014).
- ⁸⁶O. V. Dorofeeva and M. A. Filimonova, *J. Chem. Thermodyn.* **126**, 31 (2018).
- ⁸⁷E. Paulechka and A. Kazakov, *J. Phys. Chem. A* **121**, 4379 (2017).
- ⁸⁸B. Ruscic, *Int. J. Quantum Chem.* **114**, 1097 (2014).
- ⁸⁹G. N. Simm, J. Proppe, and M. Reiher, *CHIMIA* **71**, 202 (2017).
- ⁹⁰P. Pernot and A. Savin, *J. Chem. Phys.* **148**, 241707 (2018).
- ⁹¹A. J. Thakkar and T. Wu, *J. Chem. Phys.* **143**, 144302 (2015).
- ⁹²T. Wu, Y. N. Kalugina, and A. J. Thakkar, *Chem. Phys. Lett.* **635**, 257 (2015).
- ⁹³P. Pernot and A. Savin, *J. Chem. Phys.* **152**, 164108 (2020).
- ⁹⁴A. Savin and E. R. Johnson, "Judging density-functional approximations: Some pitfalls of statistics," in *Density Functionals: Thermochemistry*, edited by E. R. Johnson (Springer International Publishing, Cham, 2015) pp. 81–95.
- ⁹⁵J. P. Perdew, J. Sun, A. J. Garza, and G. E. Scuseria, *Z. Phys. Chem.* **230**, 737 (2016).
- ⁹⁶A. Gramacki, *Nonparametric kernel density estimation and its computational aspects* (Springer, 2018).
- ⁹⁷P. Winget and T. Clark, *J. Comp. Chem.* **25**, 725 (2004).
- ⁹⁸J. Cioslowski, M. Schimeczek, G. Liu, and V. Stoyanov, *J. Chem. Phys.* **113**, 9377 (2000).
- ⁹⁹M. Jaidann, S. Roy, H. Abou-Rachid, and L.-S. Lussier, *J. Hazard. Mater.* **176**, 165 (2010).
- ¹⁰⁰L. Türker, S. Gümüş, and T. Atalar, *J. Energ. Mater.* **28**, 139 (2010).
- ¹⁰¹J. P. Guthrie, *J. Phys. Chem. A* **105**, 9196 (2001).
- ¹⁰²N. Rösch and S. Trickey, *J. Chem. Phys.* **106**, 8940 (1997).
- ¹⁰³D. J. Tozer and F. De Proft, *J. Phys. Chem. A* **109**, 8923 (2005).
- ¹⁰⁴R. Ramakrishnan, A. V. Matveev, and N. Rösch, *Chem. Phys. Lett.* **468**, 158 (2009).
- ¹⁰⁵C. Spearman, *Am. J. Psychol.* **15**, 72 (1904), Reprinted: *Int. J. Epidemiol* 2010;39:1137–50.
- ¹⁰⁶J. M. Martin, *Theor. Chem. Acc.* **97**, 227 (1997).
- ¹⁰⁷J. M. Martin, *Chem. Phys. Lett.* **259**, 669 (1996).
- ¹⁰⁸J. Martin, *J. Chem. Phys.* **97**, 5012 (1992).
- ¹⁰⁹J. M. Martin, *J. Chem. Phys.* **100**, 8186 (1994).
- ¹¹⁰J. A. Pople, M. Head-Gordon, D. J. Fox, K. Raghavachari, and L. A. Curtiss, *J. Chem. Phys.* **90**, 5622 (1989).
- ¹¹¹L. A. Curtiss, K. Raghavachari, G. W. Trucks, and J. A. Pople, *J. Chem. Phys.* **94**, 7221 (1991).
- ¹¹²L. A. Curtiss, K. Raghavachari, P. C. Redfern, V. Rassolov, and J. A. Pople, *J. Chem. Phys.* **109**, 7764 (1998).
- ¹¹³S. Grimme, M. Steinmetz, and M. Korth, *J. Org. Chem.* **72**, 2118 (2007).
- ¹¹⁴S. Luo, Y. Zhao, and D. G. Truhlar, *Phys. Chem. Chem. Phys.* **13**, 13683 (2011).
- ¹¹⁵K. W. Sattelmeyer, J. Tirado-Rives, and W. L. Jorgensen, *J. Phys. Chem. A* **110**, 13551 (2006).
- ¹¹⁶A. Karton and J. M. Martin, *Mol. Phys.* **110**, 2477 (2012).
- ¹¹⁷G. Tasi, R. Izsák, G. Matisz, A. G. Császár, M. Kállay, B. Ruscic, and J. F. Stanton, *ChemPhysChem* **7**, 1664 (2006).
- ¹¹⁸P. Pernot, B. Huang, and A. Savin, *Mach. Learn.: Sci. Technol.* **4**, 1, 035011 (2020).
- ¹¹⁹B. Chan, J. Deng, and L. Radom, *J. Chem. Theory Comput.* **7**, 112 (2010).
- ¹²⁰B. Chan, A. Karton, and K. Raghavachari, *J. Chem. Theory Comput.* **15**, 4478 (2019).
- ¹²¹E. Semidalas and J. M. Martin, *J. Chem. Theory Comput.* (2020), 10.1021/acs.jctc.0c00189.
- ¹²²F. Pfeiffer, G. Rauhut, D. Feller, and K. A. Peterson, *J. Chem. Phys.* **138**, 044311 (2013).
- ¹²³K. A. Peterson, D. Feller, and D. A. Dixon, *Theor. Chem. Acc.* **131**, 1079 (2012).
- ¹²⁴V. Barone, *J. Chem. Phys.* **122**, 014108 (2005).
- ¹²⁵R. Ramakrishnan and G. Rauhut, *J. Chem. Phys.* **142**, 154118 (2015).

- ¹²⁶L. A. Curtiss, K. Raghavachari, P. C. Redfern, and J. A. Pople, *J. Chem. Phys.* **106**, 1063 (1997).
- ¹²⁷M. Chase, C. Davies, J. Downey, D. Frurip, R. McDonald, and A. Syverud, "NIST-JANAF Thermochemical Tables (ver. 1.0), online, standard reference data program; national institute of standards and technology: Gaithersburg, md, usa, 1985," .
- ¹²⁸D. Trogolo and J. S. Arey, *Phys. Chem. Chem. Phys.* **17**, 3584 (2015).
- ¹²⁹J. Cox, D. D. Wagman, and V. A. Medvedev, *CODATA key values for thermodynamics* (Chem/Mats-Sci/E, 1989).
- ¹³⁰P. M. Mayer, J.-F. Gal, and L. Radom, *Int. J. Mass Spectrom. Ion Processes* **167**, 689 (1997).
- ¹³¹B. Ruscic, M. Schwarz, and J. Berkowitz, *J. Chem. Phys.* **92**, 1865 (1990).
- ¹³²D. Wagman, W. Evans, V. Parker, and R. Schumm, *J. Phys. Chem. Ref. Data* **11** (1982).
- ¹³³D. Feller, M. Vasiliu, D. J. Grant, and D. A. Dixon, *J. Phys. Chem. A* **115**, 14667 (2011).
- ¹³⁴R. Binning Jr and L. A. Curtiss, *J. Chem. Phys.* **92**, 1860 (1990).
- ¹³⁵L. Wang, *Int. J. Mass Spectrom.* **264**, 84 (2007).